A BIOMECHANICAL INVESTIGATION OF FUSIONLESS GROWTH MODULATION IMPLANTS FOR SPINAL SCOLIOSIS TREATMENT

Nabeel Senussi Sunni (MBChB)

Principal Supervisor: Clayton Adam, Associate Professor QUT

Associate Supervisors: Mark Pearcy (Professor QUT), Geoff Askin (Adjunct Professor), Rob Labrom (Adjunct Associate Professor)

Submitted in fulfilment of the requirements for the degree of

Master of Engineering (Research)

Science and Engineering Faculty

Queensland University of Technology

2015

Keywords

Adolescent, biomechanics, bovine, calf, endoscopy, functional spinal unit, fusionless, growth modulation, hemiepiphysiodesis, idiopathic scoliosis, vertebral body staples, micro-computed tomography, spinal motion segment, scoliosis, shape memory alloy, spine, staple, stiffness, surgery, thoracic, thoracoscopic, vertebra.

Acknowledgments

I would like to acknowledge the support of everyone in the Mater Paediatric Spine Research Team. Specifically I would like to thank Clayton Adam and Mark Pearcy for their guidance, encouragement and assistance to navigate the hurdles of this academic undertaking. Thank you for believing in me till the end.

To Geoffrey Askin and Robert Labrom who provided me with a unique opportunity and mentorship. I will always appreciate what it means to have the support of two experienced senior paediatric spine surgeons. I have learnt so much working with you. Thank you.

To Maree Izatt I would like dedicate a big thank you for your patience and understanding. Your assistance was invaluable in every step of the way.

I would like to thank Beau Brooker for all the effort he put in this project. Your help in setting up the tests and Micro CT was crucial for this project. I will always remember the long days and nights of testing.

I would also like to thank all the helpful staff at MERF and IHBI who were always supportive and generous with their time to assist me.

And last but not least, I would like to thank my loving wife Saniyya, who endured the hardship of living away and was always there for me full of support and love. Thank you for inspiring me to be the best person I can be.

Abstract

Scoliosis is a common condition affecting the growing spine. It has many implications for the child's physical, mental and social development. Treatment aims include halting deformity progression, correcting the deformity, maintaining spine mobility and allowing normal growth and development. Current modes of treatment are mainly in the form of non-operative bracing and, in the case of ongoing deformity progression despite conservative treatment, surgical correction and intervertebral fusion. Each of these treatment methods compromises one or more treatment aims. Bracing is not effective in all patients, and spinal fusion permanently reduces mobility in the intervertebral joints. In an attempt to overcome these challenges, 'fusionless' scoliosis surgery techniques have emerged. These techniques involve surgical placement of an implant which attempts to provide modest deformity correction and prevent further progression, while leaving the intervertebral joints unfused. Because fusionless techniques are relatively recent, little is known about the biomechanical aspects of their correction mechanisms, which are an important determinant of treatment outcomes. The focus of this study is the biomechanics of anterior vertebral body stapling, one such technique that involves placing a two or four pronged staple across the intervertebral joint with the aim of arresting growth on the convex side of the scoliotic curve.

The study was designed with three main aims:

- First, to assess the effect of vertebral body staple insertion on spine motion segment stiffness using moment controlled mechanical testing.
- Second, to assess the tissue disruption caused by vertebral body staple insertion, in the vicinity of the staple, using Micro-Computed Tomography.
- Third, to compare the results from two different staple designs (Shape Memory Alloy and Prototype) manufactured by Medtronic Sofamor Danek (Memphis TN, USA).

The biomechanical testing in Aims 1 and 3 was performed using thoracic spines from 6-8 week old calves divided into individual motion segments and mounted onto a custom made jig attached to an Instron Biaxial Testing Machine (Instron, 8874, Norwood, Massachusetts, USA). The segments were

tested in each of the three main axes of movement (flexion/extension, lateral bending and axial rotation) under moment control. For each test, 14 motion segments were used. Testing was conducted in an environmental chamber kept at 37^{o} C and 100 % relative humidity.

The first testing program showed that insertion of the vertebral body staple resulted in a decrease in motion segment stiffness of 3% in flexion/extension, 21% in lateral bending and 11% in axial rotation.

The micro-computed tomography study showed that vertebral body staples caused epiphyseal damage, effectively causing a hemiepiphysiodesis. However, this damage was not constant, with only half of the segments showing involvement of the epiphysis on both the cephalic and caudal epiphyseal plates, and the remaining segments with one or even no epiphyseal damage. It also showed that the structural damage to the trabecular bone, following staple removal, had occurred on the outer surface of the staple prongs, indicating that it was a result of staple insertion rather than subsequent loading of the motion segment.

The biomechanical comparison between an existing commercial staple and the prototype design revealed no significant difference between the performance of the two staple designs or in the patterns of trabecular bone damage caused by staple insertion.

These findings have clinical implications in scoliosis treatment due to the fact that vertebral body stapling achieves its clinical effect by hemiepiphysiodesis and unilateral growth arrest. If physeal preservation is of importance in the course of treatment, a different fusionless scoliosis correction technology should be used.

Statement of Original Authorship

The work contained in this thesis has not been previously submitted to meet requirements for an award at this or any other higher education institution. To the best of my knowledge and belief, the thesis contains no material previously published or written by another person except where due reference is made.

Signature: QUT Verified Signature

Date: November 2015

List of Figures

LIST OF TABLES

TABLE OF CONTENTS

1. INTRODUCTION

Adolescent Idiopathic Scoliosis (AIS) is a common condition affecting 2.5% of the general population (Kane, 1977). Current mainstream methods of treatment have been limited to non-operative treatment, in the form of bracing, and operative treatment, in the form of surgical correction with spinal instrumentation and fusion. For the growing child both methods of treatment have serious implications. Bracing, although less invasive, has a high failure rate with about a third of the curves continuing to progress. This is in addition to the poor compliance rates and the psychological stigma related to wearing a brace for a prolonged period of time (years) in the child's formative years (Noonan et al., 1996, Clayson et al., 1987). Spinal instrumentation and fusion, on the other hand, is an invasive procedure that results in significant increase in the stiffness of the spine and carries a high perioperative risk in addition to the risk of adjacent level disc degeneration in the years following the operation (Coe et al., 2006).

Vertebral body stapling (Figure 1) was introduced in the early to mid-2000s as a method of treatment for AIS with moderate scoliosis (Cobb angles of 20-40 degrees), and is claimed to be a more effective alternative than bracing and less invasive than fusion (Lavelle et al., 2011). The principle of vertebral body stapling is to allow growth and movement of the vertebrae while controlling the deformity by inserting a series of metallic staples that bridge the physeal end plates and discs on the convex side of the scoliotic deformity.

FIGURE 1: EXAMPLE OF INSERTED VERTEBRAL BODY STAPLES IN SITU

Hueter & Volkmann state: "The rate of epiphyseal growth is affected by pressure applied to its axis. Compression forces inhibit growth and tensile forces stimulate growth" (Hueter, 1862, Volkmann, 1862). Aronsson *et al.* (Aronsson et al., 1999) demonstrated this on a calf's tail vertebra in 1999. It was found that when using 30-50N (5% body weight), 68% of normal growth occurred with compression, and 123% growth with distraction. This was confirmed by Stokes *et al.* in 1991 (Stokes et al., 2002, Stokes et al., 1996) as well as showing that compression caused more growth modulation than distraction. In 2005 (Stokes et al., 2005), he also showed that more modulation occurred if the force was applied for 24hrs a day as opposed to diurnal (for twelve hours a day only) application.

Based on these findings, Braun *et al.* in 2004 (Braun et al., 2004), confirmed that Shape Memory Alloy (SMA) staples are efficient in correcting moderate to severe curves as well as halting malignant scoliosis in goats. However in 2006 (Braun et al., 2006a), again using a goat model, he claimed that SMA staples showed no significant difference from the control group, whereas there was significant reduction in scoliosis using bone anchors and a synthetic ligament tether. In a further study (Braun et al., 2006b) the same group showed that SMA staples resulted in significantly less progression of scoliotic deformity compared to controls.

Betz *et al.* in 2003 and 2005, revealed in a retrospective clinical series study, that SMA staples had a better success rate than bracing in controlling and stabilising AIS as well as being a feasible and safe

method of treatment (Betz et al., 2005, Betz et al., 2003). Given the fact that fusionless scoliosis correction aims to control growth and movement of the spine by biomechanical means, it is surprising that few studies have attempted to address the effect which these treatments have on the biomechanics of the spine.

Using a moment controlled loading mechanism, Puttlitz *et al.* in 2007 (Puttlitz et al., 2007) tested the biomechanics of calf spines treated with SMA staples in 4 configurations (single prong staple positioned laterally, double prong staple positioned laterally, and then each of these with an additional single prong staple positioned anteriorly). This resulted in significantly reduced axial rotation and lateral flexion of the calf spine motion segment. The addition of an anterior staple further increased spine flexion/extension stiffness for both single and double-pronged lateral staples (P=0.02, P=0.04 respectively). The use of calf spines as a valid biomechanical analogue for human spines finds support in the work of Swartz (1991) (Swartz et al., 1991, Wilke et al., 1997), who demonstrated that the 6-8 week old calf spine is comparable to the young non-osteoporotic human spine.

Again using calf spines in an *in vitro* study, Shillington (Shillington et al., 2011) demonstrated that SMA staples do not increase stiffness of the motion segment and that the growth modulation observed following staple insertion may be due to tissue (physeal) damage by the staple tips. In this study, displacement controlled loading on a single spinal functional unit was used, however, moment controlled displacement is debated to better resemble *in vivo* circumstances. Also, the observation of damage to the physis was based on micro-CT scanning of only one of the motion segments in the study.

The overall aim of the present study is to address some of the questions raised from the previous study (Shillington et al., 2011). The specific aims of the present investigation are to:

- Assess the effect which vertebral body staples have on the stiffness of the thoracic vertebral motion segment in flexion, extension, lateral bending and rotation in a more physiological context (i.e. under moment, rather than displacement controlled testing).
- Determine the effect of the following test environment variables on motion segment stiffness

- The magnitude of applied moment necessary to achieve a physiologically representative range of motion in each main axis (flexion/extension, lateral bending and axial rotation) for the tested motion segments.
- The effect of cyclic loading on the stiffness of the motion segment.
- The effect which preservation or removal of the costovertebral joints has on motion segment stiffness.
- The effect of repeated freezing/thawing between test sequences on the mechanical properties of vertebral motion segments.

- Assess the damage to the vertebral structure caused by the insertion of a staple to the motion segment.
- Compare the results obtained with two different staple designs.

Chapter two presents the available literature, first describing the spine anatomy and biomechanics; then it goes on to describe the condition of concern, scoliosis, growth modulation, the use of bovine spine testing model and the specifics of biomechanical testing and testing environment. Finally it describes the use of vertebral body staples and the different designs available. Chapter three describes the specimens used, the preparation and testing methods for this project with details on each study phase. Chapter four presents the findings and analysis results from each study component. Chapter five discusses the findings of this study and relates them to current knowledge. Chapter six highlights the important findings of this study and how they further our understanding of spine biomechanics. It also presents some recommendations for further work.

2. LITERATURE REVIEW

2.1. THORACIC SPINE ANATOMY AND BIOMECHANICS

2.1.1. THORACIC SPINE ANATOMY

The human spine forms the central axis of the human skeleton. It provides attachment and support to the skull, thoracic cage, shoulder and pelvic girdles. It gives protection to the spinal cord which runs along its cavity. It is a complex structure combining great strength and flexibility. This is achieved by a combination of a strong bony structure and multiple closely positioned joints which are supported by a multitude of ligaments with different characteristics and a number of muscle groups (Last and McMinn, 1994).

The vertebral column (bony spine) consists of 33 vertebrae (Figure 2). These are divided into five groups, each with specific characteristics. These groups are: the Cervical, Thoracic, Lumbar, Sacral and Coccygeal vertebrae. There are 7 Cervical, 12 Thoracic, 5 Lumbar, 5 Sacral and 4 Coccygeal vertebrae (Rothman and Simeone, 1992).

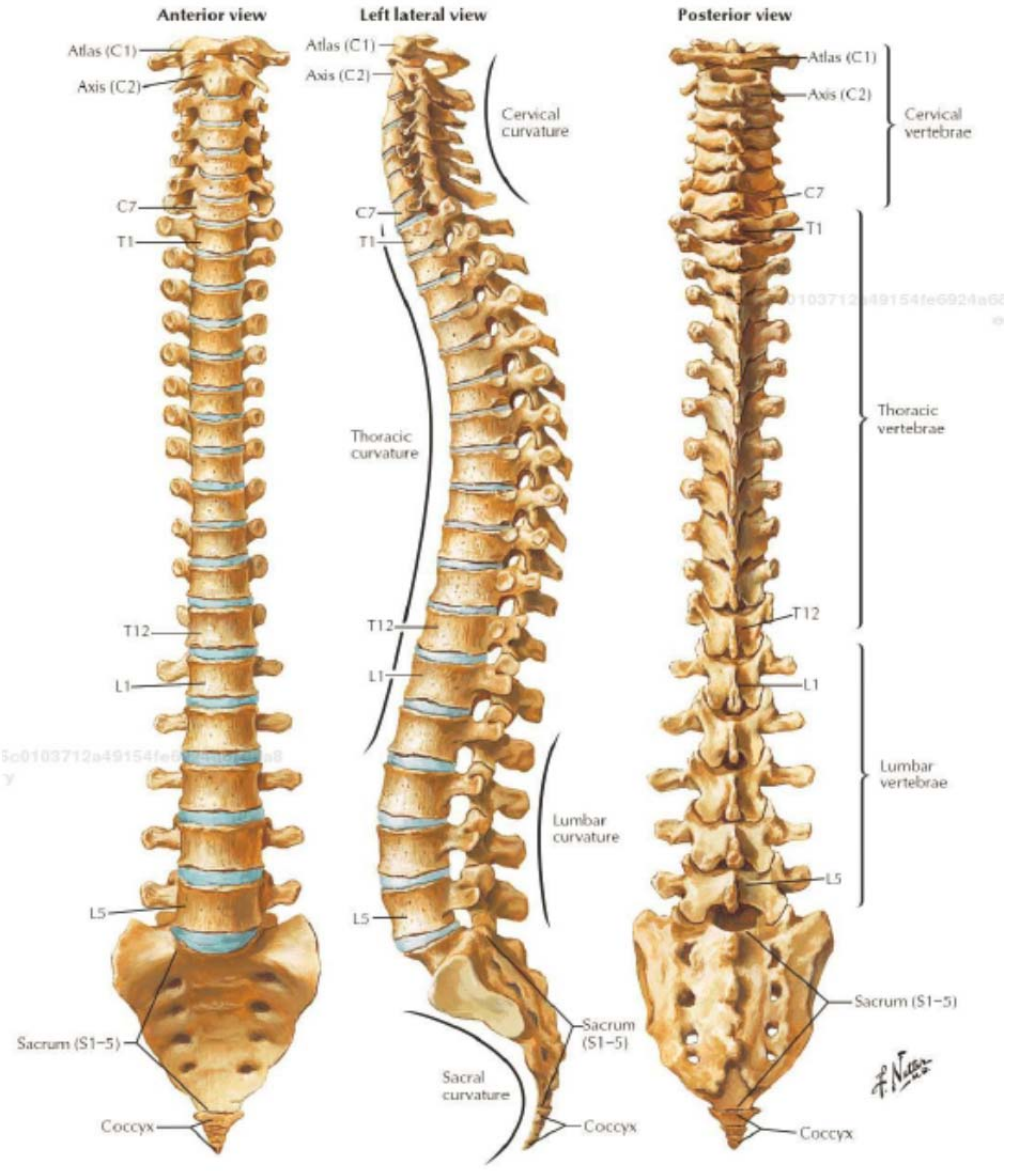

FIGURE 2: DIAGRAM OF THE HUMAN SPINAL COLUMN SHOWING THE BONY ANATOMY AND OVERALL ALIGNMENT AND DIFFERENT REGIONS. (NETTER, 2010).

Each vertebra (Figure 3) is made up of a body anteriorly, and a neural arch posteriorly. Between the body and the neural arch is a large foramen: the vertebral foramen, through which the spinal cord passes. The body is the vertical load bearing part of the vertebra. The neural arch is made up of the pedicles and laminae and gives rise to 3 processes. In the posterior midline is the spinous process and on either side a transverse process. The size and shape of these components differs from one group of vertebrae to another as each group has its own characteristic features.

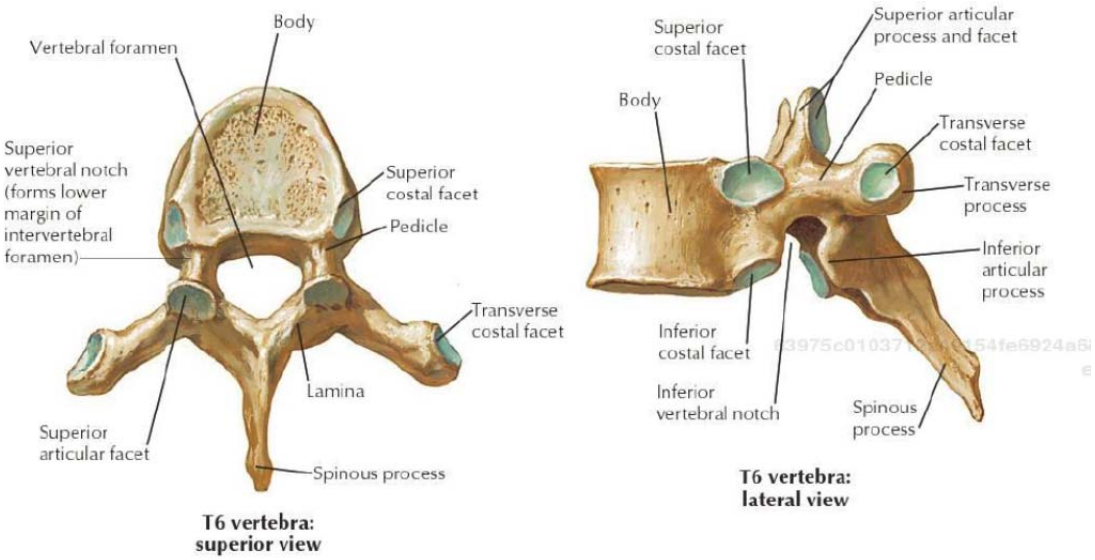

FIGURE 3: ANATOMY OF A TYPICAL THORACIC VERTEBRA (NETTER, 2010).

The vertebrae are held together by a complex combination of joints and ligaments that allow specific movements in each group. Generally there is a greater degree of movement between the neural arches than between the vertebral bodies.

The vertebral bodies are held together by the intervertebral discs which are composed of a thick fibrous outer layer: the anulus fibrosus; and an inner gelatinous substance: the nucleus pulposus. This allows the intervertebral joints to support large axial loads while offering a degree of flexibility and movement. In addition to the intervertebral discs the vertebral bodies are connected by the anterior and posterior longitudinal ligaments.

The neural arches articulate with the vertebrae above and below through the zygapophysial joints. The zygapophysial joints are also known as facet joints, as they are formed by the articulation of the left and right inferior facets of the vertebra above and the corresponding left and right superior facets of the vertebra below. These allow gliding movements in specific axes, which differ from one region of the spine to another. The capsules of these joints provide an element of stability to the spine. In addition to the facet joints, posterior stability is also provided by the ligamenta flava, which connect the contiguous lamina, the supraspinous ligaments, intertransverse ligaments and the interspinous ligaments.

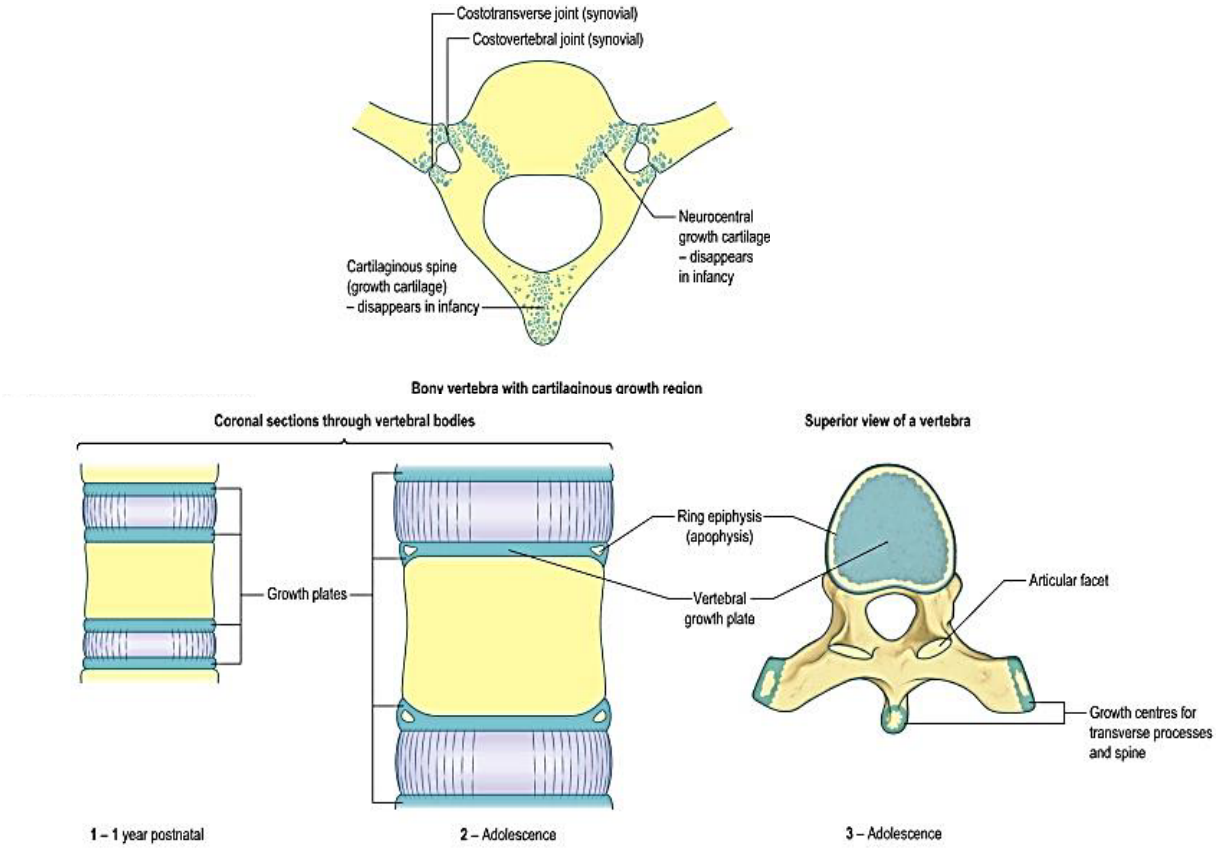

FIGURE 4: EPIPHYSEAL PLATES OF THE VERTEBRAL BODY(STANDRING, 2008)

In addition to the above characteristics the thoracic vertebrae articulate with the ribs at the costovertebral and costotransverse joints. Each rib articulates with its own vertebral body, the vertebral body above, and the intervertebral disc between them by a synovial joint. This synovial joint is surrounded by a capsule and is attached to the vertebral body anteriorly by the radiate ligament. The tubercle of each rib also articulates with the transverse process of its respective vertebra by another synovial joint and its surrounding capsule. The rib is attached to the transverse process by the medial and lateral costotransverse ligaments, which provide additional stability in the thoracic region.

The immature spine also has epiphyseal plates (growth plates) superiorly and inferiorly at the superior and inferior ends of the vertebral body as well as growth plates in the transverse processes and spinous processes (Figure 4).

The vertebral column typically has a cervical lordosis, thoracic kyphosis, lumbar lordosis and sacrococcygeal kyphosis. All these curvatures are only in the sagittal plane. The normal spine does not have any lateral (left or right) curvatures (Figure 2).

2.1.2. BIOMECHANICS OF THE THORACIC SPINE

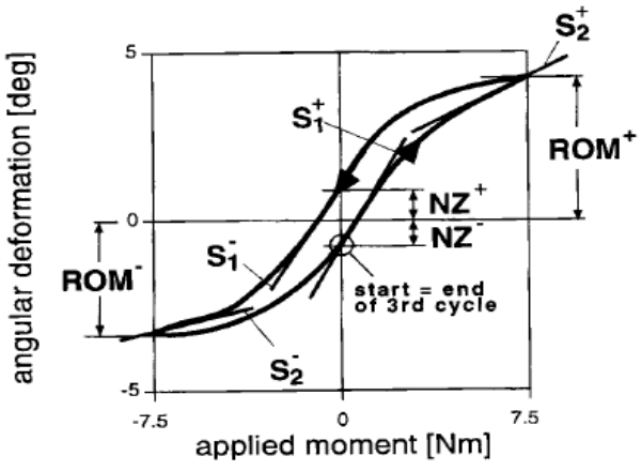

FIGURE 5: TYPICAL LOAD-DISPLACEMENT CURVE. ROM = RANGE OF MOTION, NZ= NEUTRAL ZONE (WILKE ET AL., 1996).

Spinal motion segments have a distinctive two phase load-displacement curve (Figure 5). In the initial phase large degrees of rotation are achieved by small moments. There is a change to the second phase in which large forces are necessary to achieve a relatively small rotation (Wilke et al., 1998b, Gilbertson et al., 2000).

The smallest segment of spine that exhibits the biomechanical characteristics similar to those of the entire spine is known as the Functional Spinal Unit or Motion Segment (Rothman and Simeone, 1992). It consists of two adjacent vertebrae and connecting ligaments. In the thoracic region this includes the costovertebral articulations.

The thoracic spine is of particular interest as it is most common site for the major scoliotic curve and is therefore the focus of this thesis (Moe and Kettleson, 1970, Gore et al., 1981). The range of motion (ROM) in the human thoracic spine depends on the level measured and the main axis of movement.

In the upper thoracic segments the average ROM in flexion/extension is 4^0, 6^0 in the middle segments and 12^0 in the lower segments. In lateral bending the upper segments have a ROM of 6^0 and increase to 9^0 in the lower segments. The ROM for axial rotation ranges from 9^0 in the upper segments to 2^0 in the lower segments (Panjabi et al., 1976, Panjabi and White, 1980).

2.2. SCOLIOSIS

2.2.1. INTRODUCTION:

FIGURE 6: EXAMPLE OF THE CLINICAL APPEARANCE OF IDIOPATHIC SCOLIOSIS.

Scoliosis is defined as a lateral curvature of the spine with a Cobb angle equal to or more than 10 degrees. This is an oversimplified definition that takes into account the deformity appearance in the coronal plane only. However, scoliosis is a three dimensional deformity with a degree of coronal deformity, sagittal deformity and axial or rotational deformity (Stokes, 1994) (Figure 6). Scoliosis can be either secondary to a known cause, such as congenital deformities, neurological or neuromuscular disorders, or when no primary cause can be identified it is known as idiopathic scoliosis. This forms 80% of all scoliosis cases (Herkowitz et al., 2011). Traditionally idiopathic scoliosis was divided chronologically into infantile (0 to 3 years of age), juvenile (4 to 9 years) and adolescent (10 years to adulthood). Juvenile idiopathic scoliosis is a rare condition and the growth rate between ages 5 and 10 is slow. Therefore a common classification used is early onset (0 to 5 years) and late onset (>5 years to maturity). It is now well known that the functional development of the lungs continues after birth. As much as 90% of the adult number of alveoli are budded off in the first eight years of life (Last

and McMinn, 1994). Therefore this newer classification has significant value. This affects treatment decisions and intervention modalities based on the age of the patient with the aim to maximise thoracic development in the child's first eight years of life.

2.2.2. EPIDEMIOLOGY

Infantile idiopathic scoliosis occurs in less than 1% of idiopathic scoliosis cases. It occurs more commonly in males, with a male to female ratio of 3:2 (Rothman and Simeone, 1992). Most deformities appear within the first year of life. The majority (90%) have a left sided (convex to the left) curve (Frymoyer and Wiesel, 2004, Rothman and Simeone, 1992). Juvenile idiopathic scoliosis accounts for 12-21% of all idiopathic scoliosis. The male to female ratio is 1:1 with increased female predominance over the age of 6 years to reach a maximum ratio of 4:1 depending on age. Adolescent idiopathic scoliosis (AIS) is more prevalent representing 80% of idiopathic scoliosis and an overall prevalence of 2.5% of the general population (Kane, 1977). Among these, 5% go on to progress beyond 30 degrees. It is much more common in females than males. However, this is dependent on the size of the curve with an equal male to female ratio for curves around 10 degrees, increasing in females with higher curve angles, resulting in a male to female ratio of 1:4 above 10 degrees and 1:10 above 40 degrees. AIS curves are mainly right sided (convex to the right) curves (Fernandes and Weinstein, 2007, Frymoyer and Wiesel, 2004, Rothman and Simeone, 1992).

2.2.3. PATHOGENESIS

Although the exact cause of idiopathic scoliosis in not known, there are a few theories as to the mechanism of its progression. It is commonly believed that idiopathic scoliosis starts out initially as a '**functional**' deformity. During this phase the deformity is flexible and fully correctable on lateral bending. Prolonged functional deformity leads to secondary changes in vertebral shape as a result of preferential growth according to the Hueter-Volkmann Law. This is known as the vicious cycle effect (Stokes et al., 1996). As a result the deformity becomes irreversible on removal of the asymmetrical loading, and is known as a '**structural**' curve. It is believed that this vicious cycle effect is responsible for the progression of the scoliosis curve. Secondary curves appear as a compensatory measure to balance the head and trunk over the pelvis. In the same fashion, they can be either functional or

structural (Figure 7) (Mente et al., 1997, Roaf, 1960, Stokes, 2002, Hawes and O'Brien J, 2006, Harrington, 1977).

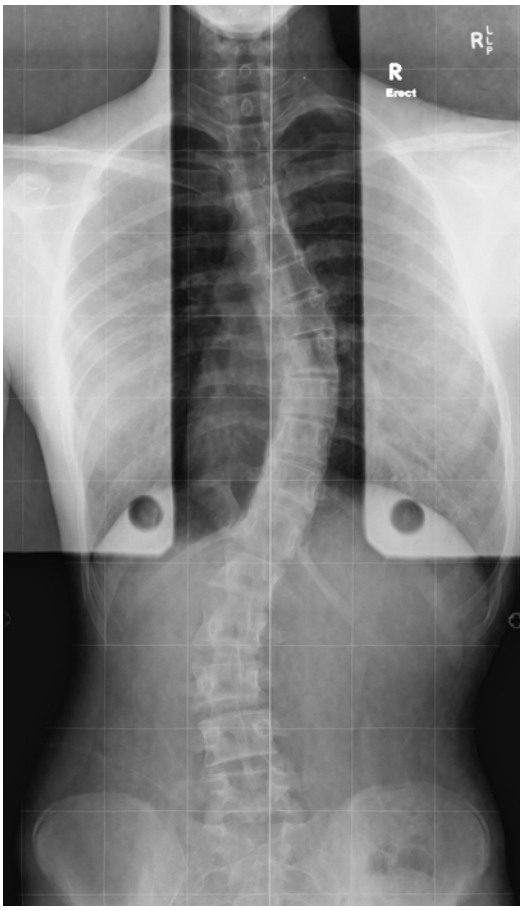

FIGURE 7: RADIOGRAPH OF A CHILD WITH SCOLIOSIS SHOWING A MAIN THORACIC CURVE AND A SECONDARY LUMBAR CURVE.

2.2.4. NATURAL HISTORY:

Up to 90% of infantile idiopathic scoliosis curves resolve spontaneously, especially if they present before one year of age (Lloyd-Roberts and Pilcher, 1965). The curves most likely to progress are the double curves or later presentation. Juvenile curves have a 70% progression rate; however, curves with a Cobb angle of less than 25 degrees have a tendency to resolve (Diedrich et al., 2002, Lenke and Dobbs, 2007).

AIS progression is affected by many factors including age of onset, growth potential, skeletal maturity, angle of curve, location of curve and number of curves involved to mention a few. Curves are more

likely to progress around the time of peak height growth and in the case of double curves. After maturity the curve is likely to progress if it is thoracic with a Cobb angle of 50 degrees or greater, or thoracolumbar with a Cobb angle of 30 degrees or more (Bunnell, 1986, Rothman and Simeone, 1992, Fernandes and Weinstein, 2007).

2.2.5. PRESENTATION:

Most presentations are either through school screening programs, noticed by family, general practitioner or paediatrician. Usually the first signs noticed are uneven shoulder level, waistline asymmetry and thoracic or lumbar hump. Occasionally symptoms of back or shoulder pain or weakness are present.

Clinical assessment is centred on excluding a primary cause and assessing the degree of the deformity. The deformity is measured from an erect posteroanterior, full length, thoracolumbosacral spine x-ray. A lateral spine x-ray is also performed to assess for any kyphosis. The Cobb angle technique is used to measure the angle. This is defined as the angle created between a line drawn parallel to the superior endplate of the highest vertebra of the curve (the most tilted) and a line drawn parallel to the inferior end plate of the lowest vertebra of the curve (the most tilted) (Cobb, 1948). The rib hump is measured with a scoliometer and offers information regarding the rotation of the vertebrae.

2.2.6. TREATMENT

Management depends on the severity of the curve, the age of the child and the likelihood of progression of the curve. The treatment options can be divided into non-operative and operative treatment.

2.2.6.1. NON-OPERATIVE TREATMENT:

This can be in the form of:

- Observation with regular monitoring (both clinical and radiological) to assess any degree of progression and its rate.

- Bracing, which can involve the use of one of many devices ranging from plaster of Paris casts to the Milwaukee or Boston (thoraco-lumbo-sacral and cervico-thoraco-lumbo-sacral orthoses TLSO, CTLSO), to flexible braces such as the SpineCore brace (Figure 8).

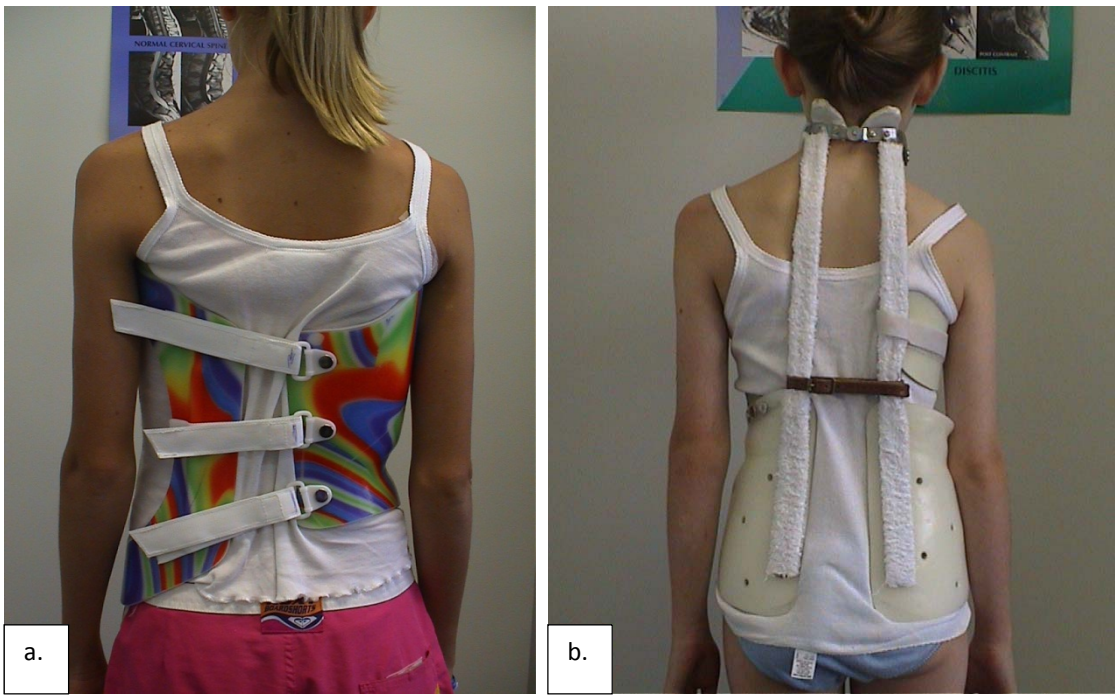

FIGURE 8: EXAMPLES OF BRACES. a. THORACO-LUMBO-SACRAL ORTHOSIS (TLSO), b. CERVICO-THORACO-LUMBO-SACRAL ORTHOSIS (CTLSO).

The main aim of non-operative treatment is to maintain an acceptable curve and prevent progression throughout growth. Therefore it is best commenced before the adolescent growth spurt. Unfortunately this is difficult to predict. The Risser score has been commonly used to help assess this. The Risser score uses the iliac crest apophysis development to determine progression to skeletal maturity. This is described on a scale of 0-5 (Hacquebord and Leopold, 2012). The development of secondary sexual characteristics and, in females, menarche are also indications of skeletal maturity and potential for curve progression. Although different surgeons and different centres have different cut off points for initiating and stopping brace treatment, the common indications are a curve of 25 – 45 degrees and Risser score of 0-1. The brace is applied for 23hrs a day. This is continued until cessation of growth (growth of less than 1 cm in 6 months, Risser score of 5 and/or 2 years post menarche). Despite this there is still a 20-40% failure rate requiring surgical intervention (Noonan et al., 1996,

Lonstein and Winter, 1994, Howard et al., 1998). This is partly due to the nature of the curve and also patient compliance. There is also a negative psychosocial effect on patients treated with braces (Wickers et al., 1977, Climent and Sanchez, 1999).

2.2.6.2. OPERATIVE TREATMENT:

This can be in the form of (Lenke and Dobbs, 2007, Maruyama and Takeshita, 2008):

- Surgical correction and intervertebral fusion.
- Surgical correction with fusionless devices.

- INTERVERTEBRAL FUSION

Surgical correction and intervertebral fusion is indicated if other treatment methods have failed to correct or control the curve, or if the deformity is severe. It is usually chosen for curves that are greater than 45 degrees in children more than 10 years old (Goldstein, 1971, James, 1971). The aim of these techniques is to achieve correction of the deformity by a magnitude of 50-70% (Goldstein, 1971, Maruyama and Takeshita, 2008, Westrick and Ward, 2011) and to maintain this correction until intervertebral arthrodesis (fusion) occurs. Fusion is achieved either through posterior intervertebral instrumentation (rods, screws and/or wires), anterior instrumentation, and combined posterior and anterior instrumentation (Figure 9). The technique was originally described by P. R. Harrington in 1962 through a posterior approach (Harrington, 1962). However, his technique has since been modified with the use of hybrid systems involving multiple pedicle screw anchoring points, hooks and sublaminar wires. Correction is achieved by a combination of concavity distraction, rod rotation and convex compression. In addition to the posterior approach, a combined anterior and posterior approach can be used for severe stiff deformities. More recently an anterolateral, minimally invasive (thoracoscopic) correction and instrumentation technique has gained popularity (Lonner, 2007). Correction is achieved by insertion of anterolateral anchoring vertebral body screws and rod construct with compression on the convex side. This is possible for mainly thoracic curves (curves where the structural scoliosis is in the thoracic region only and has a single structural curve). The advantage of minimally invasive surgery is that it is less traumatic, has quicker recovery rates, shorter hospital stay

and smaller more concealed scars (Rothman and Simeone, 1992, Frymoyer and Wiesel, 2004, Izatt et al., 2006, Lee et al., 2011).

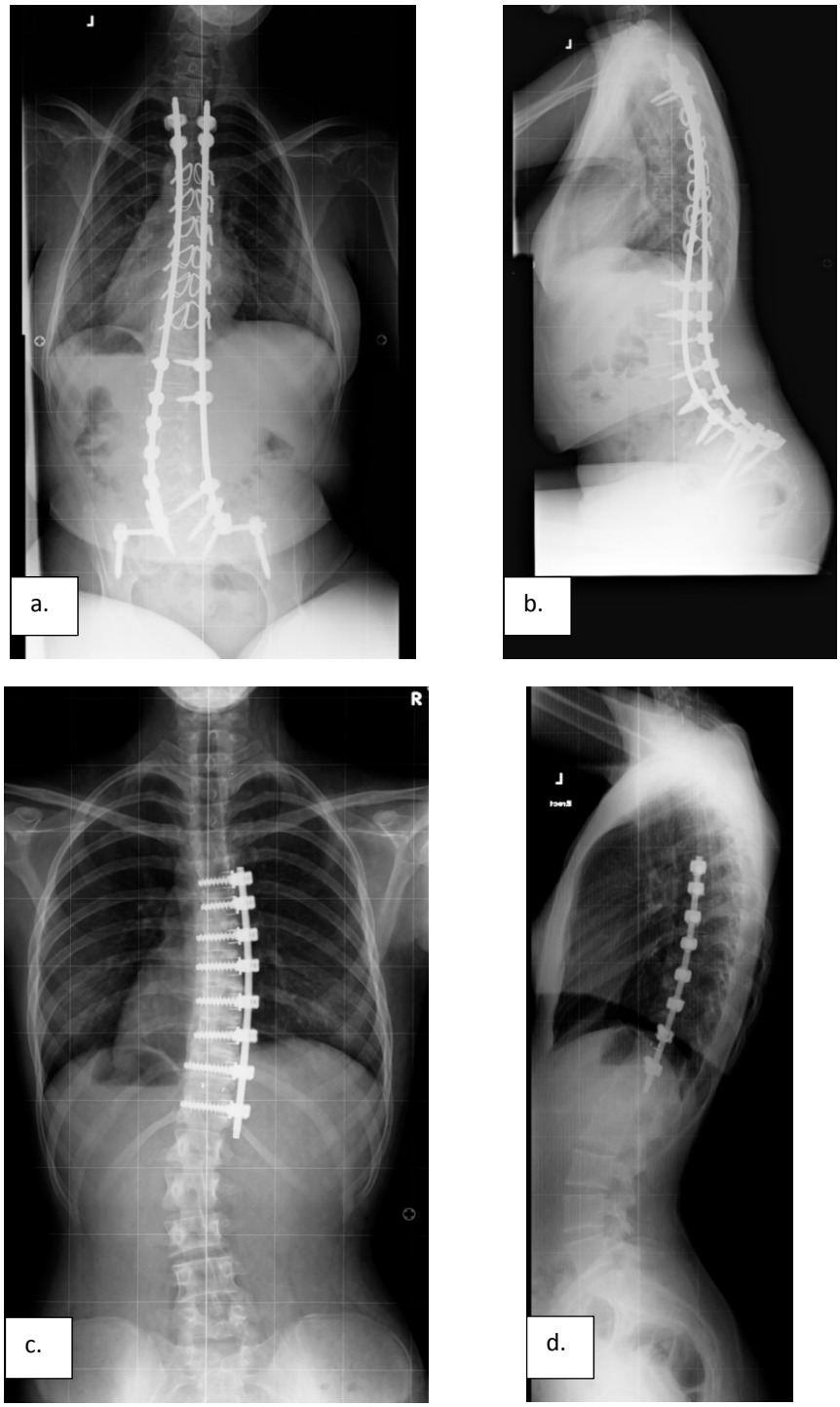

FIGURE 9: EXAMPLES OF INTERVERTEBRAL FUSION; (a., b.) POSTERIOR INSTRUMENTATION, (c., d.) ANTERIOR/ANTEROLATERAL INSTRUMENTATION.

Although highly successful, surgical correction, instrumentation and fusion permanently removes spinal flexibility across the fused levels, and there is a risk of adjacent level arthritis as well as higher

perioperative risks including infection, pneumothorax, haemothorax and paralysis (Coe et al., 2006, Cochran et al., 1983, Westrick and Ward, 2011, Geervliet et al., 2007).

- FUSIONLESS SURGERY

Recently, fusionless technologies have been developed to address some of the problems associated with intervertebral fusion (Coe et al., 2006) such as stiffness, adjacent segment arthritis and high perioperative risks involving blood loss, large volume shifts with electrolyte disturbances, prolonged surgical time, thromboembolism, hypothermia and crankshaft phenomena. Different techniques have been used; these include epiphysiodesis, posterior intervertebral growing rods, vertical expandable prosthetic titanium rib devices, anterior fusionless devices such as vertebral body staples and bone anchors with ligamentous tethers (Akbarnia, 2007, Guille et al., 2007).

McCarroll and Consten (McCarroll and Costen, 1960) described a procedure in 1960 that involved a **thoracotomy, convex rib resection and convex apical epiphysiodesis** in an attempt to correct the scoliosis curve by growth modulation. Unfortunately, their results were not satisfactory, as they failed to influence the progression of the curve. Roaf (Roaf, 1963) published a study involving convex side epiphysiodesis with a similar technique he achieved more than 10 degrees of correction in 60% of cases. He also reported a significant improvement in appearance in all the patients which resulted in high patient satisfaction. Unfortunately, although these results are promising; this technique is very invasive, as it involves an anterolateral and posterior approach to the spine, and the results were unpredictable (Marks et al., 1996, Nilsonne, 1969).

Another fusionless technique is the application of posterior **growing rods**. These are mainly used as a temporary measure for curve control to allow further growth and maturity of the patient with early-onset scoliosis. They are usually made of titanium and applied with anchors (pedicle screws and/or hooks) at the cephalic and caudal ends of the deformity with spanning rods inserted submuscularly (Figure 10). Each rod consists of two telescoping rods with a locking mechanism. They are applied with distraction on the concave side to correct the deformity. The telescoping mechanism allows for regular (six monthly or annually) adjustment by increasing the distraction applied. This allows for the child's spine to continue growing while controlling progression of the curve (Yazici and Emans, 2009).

Commonly, when the child is older, a definitive procedure is performed in the form of correction and intervertebral fusion.

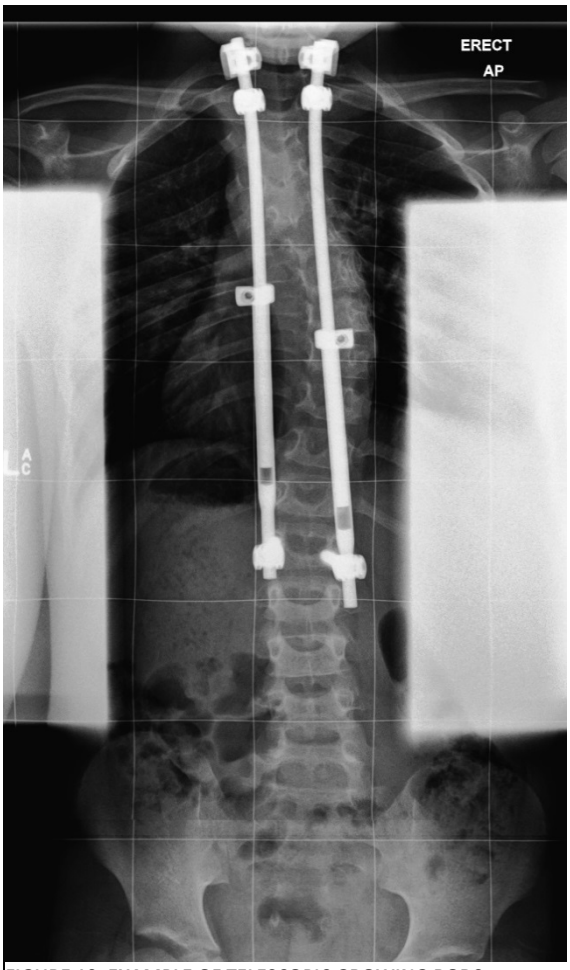

FIGURE 10: EXAMPLE OF TELESCOPIC GROWING RODS.

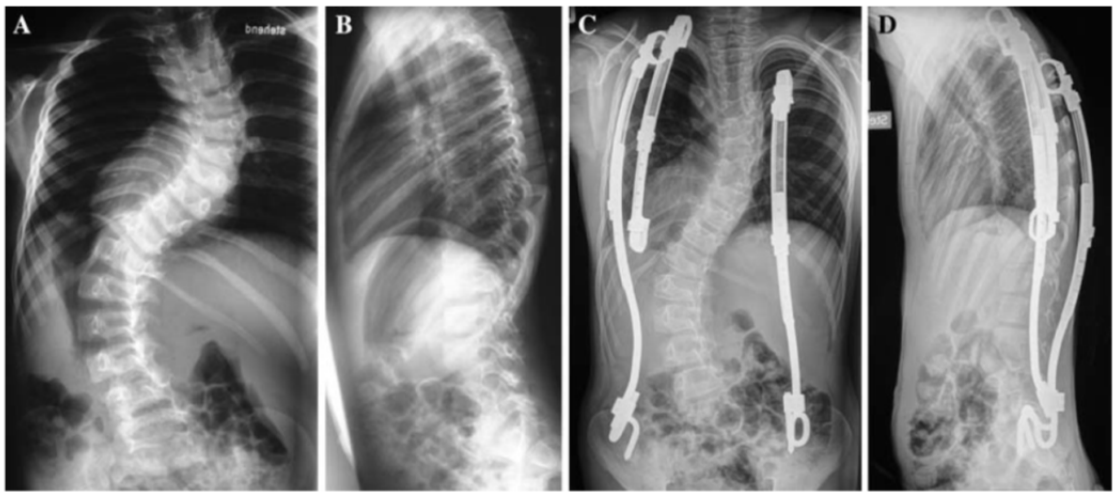

FIGURE 11: EXAMPLE OF THE USE OF VEPTR DEVICES (HASLER ET AL., 2010).

Vertical Expandable Prosthetic Titanium Rib devices (VEPTR) (Hasler et al., 2010, Campbell, 2013) are similar in principle to growing rods, however the location of application of corrective force is more lateral as it is attached to a cephalad and caudad rib or to the iliac crest (Figure 11). VEPTR implants allow for serial expansion and are designed to allow thoracic cage development as the child grows. They are specifically useful in those cases with congenital and infantile scoliosis where the deformity of the chest is severe and causing thoracic insufficiency, and can indirectly improve the scoliosis curve as well as encourage chest wall growth and expansion. VEPTR devices are used either alone or in conjunction with a growing rod. Again, as with the growing rods, the child is likely to require definitive corrective surgery and fusion at an older age.

Intervertebral flexible tethering with vertebral anchors (Figure 12) has been described in many studies involving animal models (Newton et al., 2002, Braun et al., 2003, Braun et al., 2006b, Newton et al., 2008a, Newton et al., 2008b). There have been multiple patents for such devices also. A. F. Dwyer (Dwyer et al., 1969, Dwyer, 1973) developed an anterior tethering system in 1969 using anchoring screws, hooked plates and a titanium cable. This construct, although effective in theory, has fallen out of favour due to complications, failure of the construct and inadequate correction (Dwyer, 1973, Halm, 2000, Kohler et al., 1990, Blair et al., 1993, Halm et al., 2009). Recently Braun *et al.* have compared an anterior tethering system to the performance of vertebral body staples in an animal model (Braun et al., 2005). Crawford *et al*. reported a case using anterior vertebral screws and a polypropylene tether with good results (Crawford and Lenke, 2010). Last year Samdani *et al*. published 2 year follow-up results using a flexible tether in 11 scoliosis correction cases (Samdani et al., 2014). The reported results are promising, however, as with any new technology further studies and longer term results will be needed to confirm these findings.

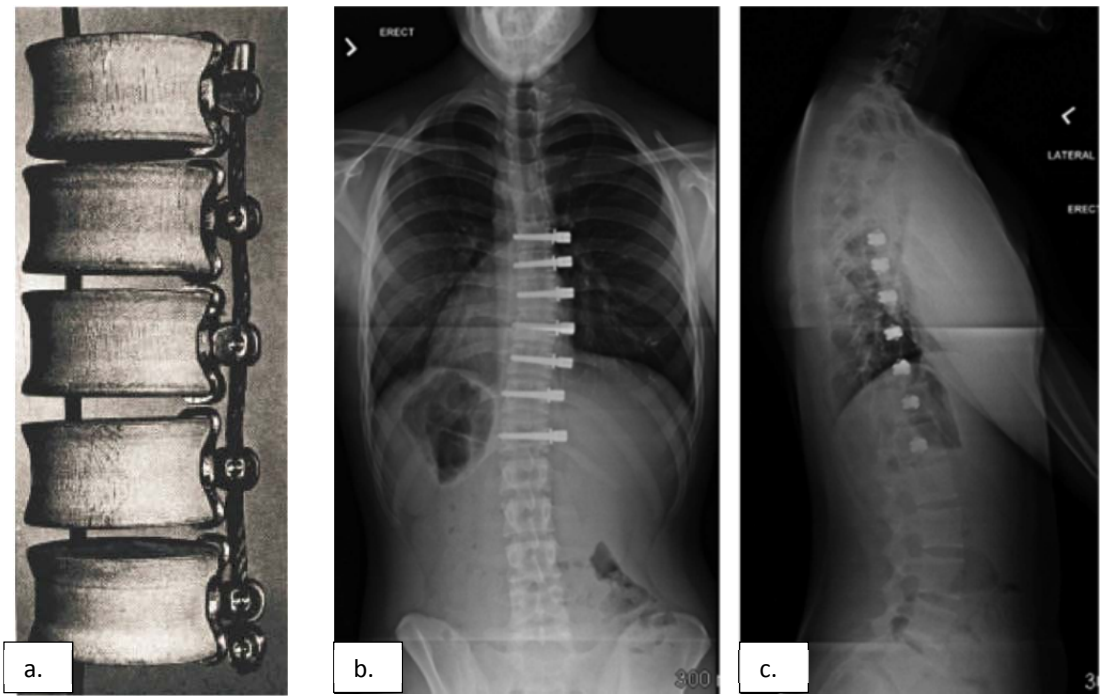

FIGURE 12: DIFFERENT TETHERING SYSTEMS. a. DWYER ET AL CONSTRUCT(DWYER ET AL., 1969), b&c. SAMDANI ET AL TETHERING SYSTEM (SAMDANI ET AL., 2014) THE TETHER IS NOT VISIBLE AS IT IS RADIOLUCENT POLYPROPYLENE.

Vertebral body stapling (Figure 13) also relies on growth modulation by attempting to slow down growth on the convex side of the curve (Betz et al., 2003, Braun et al., 2004, Betz et al., 2005, Braun et al., 2005, Braun et al., 2006b, Lavelle et al., 2011). It utilises the minimally invasive surgery techniques achievable with thoracoscopy. Vertebral body staples are indicated in girls <13yrs old and boys <15yrs old, Risser score of 0-1, coronal (scoliotic) curve of 25-45 degrees with a minimum of 50% flexibility, and <40 degrees kyphosis. Although these indications are similar to those of bracing, the patients do not wear a brace postoperatively. This addresses the psychosocial complications associated with bracing. It also has slightly better success rates of treatment (77% for thoracic curves and 83% for lumbar curves) compared to bracing (Betz et al., 2005, Guille et al., 2007, Betz et al., 2010, Lavelle et al., 2011, Trobisch et al., 2011). The staples come in two main forms, two pronged or four pronged, with the four pronged version almost exclusively used in clinical practice. This implant will be described in more detail as it is the focus of this study.

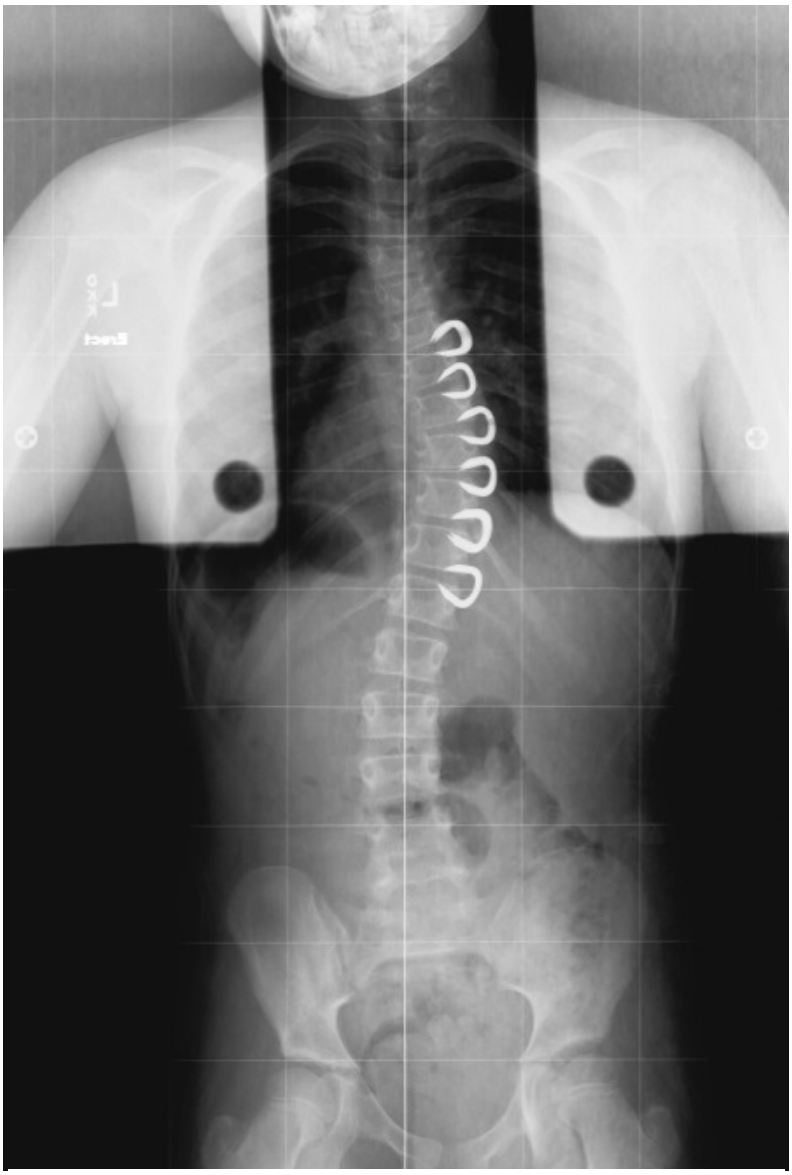

FIGURE 13: EXAMPLE OF VERTEBRAL BODY STAPLES PLACED ON THE CONVEX SIDE OF A SCOLIOTIC CURVE IN AN AIS PATIENT.

2.3. GROWTH MODULATION

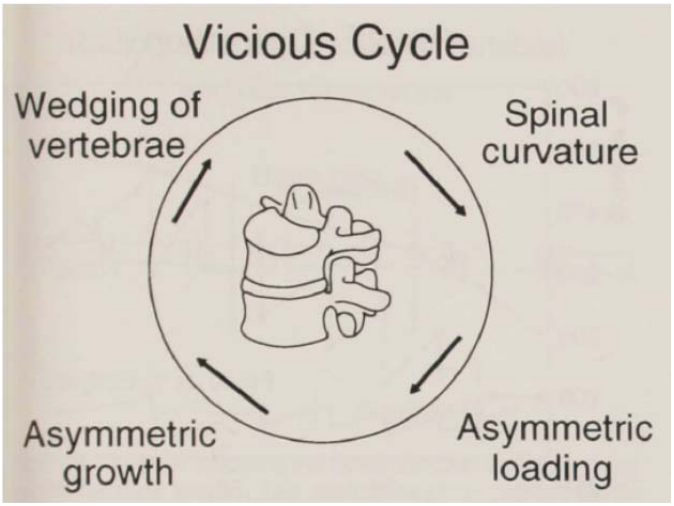

FIGURE 14: THE VICIOUS CYCLE THEORY (STOKES ET AL., 1996).

Although the cause of AIS is unknown (and probably multifactorial), it is believed that the "vicious cycle" theory is responsible for its progression (Stokes et al., 1996) (Figure 14). Epiphyseal growth plays a role in the progression of scoliosis as the fastest deformity progression occurs during the growth spurt periods. This has led to the thinking that by altering the speed of growth selectively (by slowing down the growth on the convex side of the curve) a gradual correction can be achieved. This 'growth modulation' approach is not a new approach to deformity correction. It is derived from the Hueter-Volkmann law (Risser, 1958, Stokes et al., 1996) which states that "The rate of epiphyseal growth is affected by pressure applied to its axes; compression forces inhibit growth and tensile forces stimulate growth". This principle has been used for many years in correction of other deformities such as Blount's disease (Blount and Clarke, 1949) (tibia vara). By modulating the growth on one side by compression a controlled correction can be made. This slows down the growth on the apex side of the epiphysis and allows the concave side to continue growth. The desired compression can be achieved with staples or plates and screws. Studies using animal models have shown this principle to be effective on the immature spine (Aronsson et al., 1999, Stokes et al., 2005, Akyuz et al., 2006). Aronsson *et al.* demonstrated this on a Calf's tail vertebra in 1999. It was found that using 30-50N (5% body weight) resulted in 68% of normal growth occurring with compression and 123% with distraction (Aronsson et al., 1999). Stokes *et al.* in 2002 also confirmed this as well as showing

that compression caused more growth modulation than distraction using caudal vertebrae of rats (Stokes et al., 2002). He also showed in 2005 that more modulation occurred if the force was applied for 24hrs a day as opposed to diurnal application. This was done by applying a compressible external fixator onto rat tibiae and rat tail vertebrae in four different groups, 24/24 hrs, 12/24 hrs day, 12/24 hrs night and 0/24 control. The pressure was applied evenly across the tested epiphyses (Stokes et al., 2005).

2.4. IMMATURE BOVINE SPINE MODEL

2.4.1. JUSTIFICATION FOR CHOICE OF ANIMAL MODEL:

It is difficult to obtain cadaveric human spine samples in the studied age group (adolescents), and nearly impossible to obtain a sufficient number of samples to conduct the studies outlined above. Therefor a suitable substitute had to be found (Sheng et al., 2010, Smit, 2002, Drespe et al., 2005, Kettler et al., 2007). Calf spine samples were chosen in this study due to the structural and biomechanical similarities as shown in the next section.

2.4.2. BIOMECHANICAL PROPERTIES:

Immature bovine (calf) spines are the focus of the present study because they have been shown to be a good model for the young human spine (Figure 15). Cotterill *et al.* in 1986 demonstrated that the six to eight week old calf spine is similar in length to the young human adult spine, it has greater homogeneity and almost identical facet joint orientation at levels T6 and T12 (Cotterill et al., 1986). Swartz in 1991 demonstrated that the 6-8 week old calf spine is comparable in tissue, mineral and ash density, as well as compressive strength and modulus, to the young non-osteoporotic human spine (Swartz et al., 1991). Wilke *et al.* in 1996 demonstrated that calf thoracolumbar spines had similar load displacement properties (Wilke et al., 1996) when compared to those published by Panjabi and White for the human spine. The range of motion in the human thoracic spine motion segments was described as (Panjabi and White, 1980):

a) Flex/Ext: 4 degrees in the upper 1/3, 6 degrees in the middle 1/3 and 12 degrees in the lower 1/3.
b) Lateral Bending: 6 degrees in the upper thoracic spine and 8-9 degrees in the lower T spine.
c) Axial rotation: 8-9 degrees, 2 degrees in the lower 3 segments.

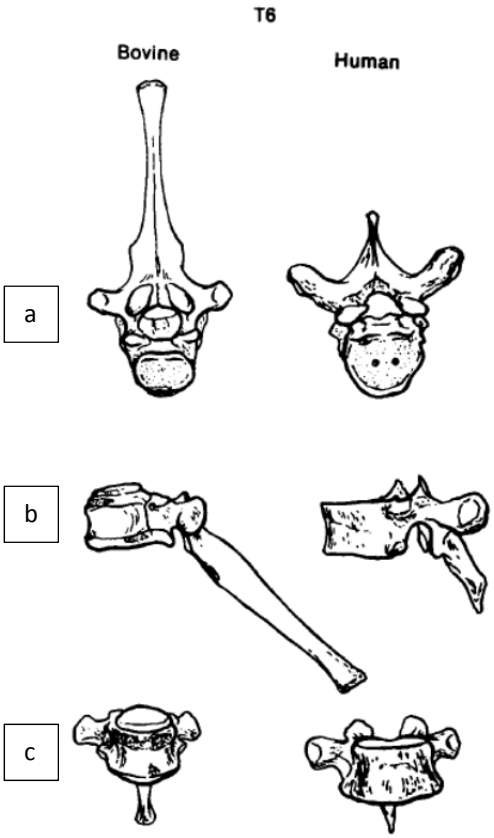

FIGURE 15: COMPARISON OF HUMAN T6 (TO THE RIGHT) AND BOVINE T6 (TO THE LEFT) VERTEBRAE FROM TOP (a), LATERAL (b) AND ANTERIOR (c) VIEWS.(COTTERILL ET AL., 1986).

2.5. BIOMECHANICAL TESTING

2.5.1. DISPLACEMENT VS LOAD CONTROL

As outlined in Section (2.1.1) the human spine is a very complex structure. In an ideal situation the spine would be studied *in vivo*. Unfortunately, past *in vivo* studies have lacked clear-cut conclusions relating to the actual biomechanics of the spine. This can be attributed to a multitude of factors affecting confounding variables such as: structural weakening, inhibition or facilitation of muscles in response to pain or discomfort. As a result, *in vitro* studies have been designed to provide a more objective biomechanical assessment of the intervention under study (Goel et al., 1995). To obtain the physical characteristics of a construct there are two choices of experimental methods. Either a *Stiffness experimental design*, which is also known as *Displacement control testing,* or *Flexibility experimental design* also known as *Moment control testing*

. In displacement control testing, the free end of the construct is displaced in a certain direction or around a predefined axis by a certain amount; the resulting forces and moments are then measured. On the other hand, in moment control testing, a specific load is applied to the construct; the displacement is then measured (Panjabi, 1988). Both methods have their advantages and disadvantages. The choice of method depends on the aim of the study.

The displacement control method is best suited for low stiffness conditions such as measurements around the neutral zone (Goel et al., 1995, Thompson et al., 2003, de Visser et al., 2007). However, it does not replicate normal spine movement with its coupled movements in the non-dominant axis or plane. On the other hand moment control testing applies a force and measures the different movements resulting from it. This is believed to resemble *in vivo* conditions more accurately. It is important to consider the type and method of force application in relation to the point of measurement. Application of pure moments involves applying a uniform moment along the whole tested segment; this results in the most consistent measurements across the whole specimen (Panjabi, 1988, Wilke et al., 1998b, Panjabi, 2007) (Figure 16).

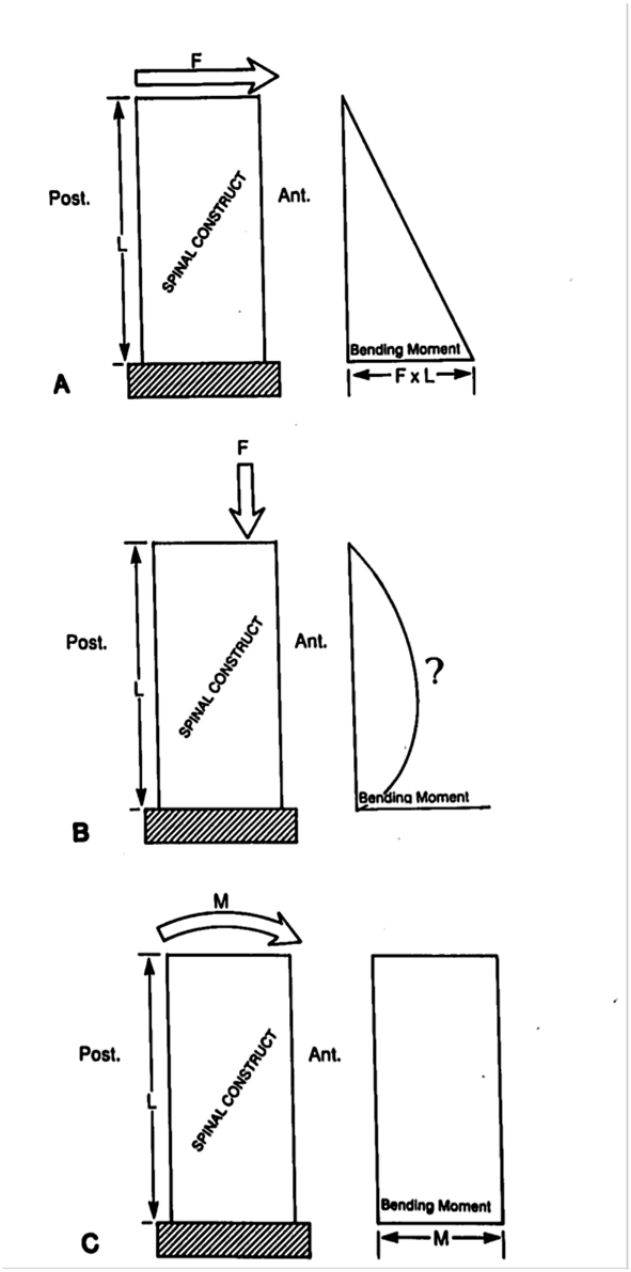

FIGURE 16: DIFFERENT METHODS OF FORCE APPLICATION AND THE RESULTANT MOMENT EXERTED ON THE TESTED SPECIMEN. a: SHEAR FORCE APPLIED, b: ECCENTRIC FORCE APPLIED AND c: PURE BENDING MOMENT (PANJABI, 1988).

A previous study from the author's team has shown the effect of vertebral body staple insertion on motion segment biomechanics using displacement control (Shillington et al., 2011). Therefore it was the aim of this study to demonstrate the effect of intervertebral insertion in a more physiologically realistic environment, using moment control, in an attempt to replicate *in vivo* conditions as closely as possible.

2.5.2. Effect of Progressive Cyclic Loading on Immature Bovine Spine Segments

During the course of an *in vitro* biomechanical test of spinal segments it is commonly necessary to perform multiple tests on the same segment. This implies a cumulative increase in the number of load cycles as testing proceeds. As this study involved testing the segments firstly un-instrumented (to measure baseline motion segment stiffness) and then retesting the same segments after the intervention, it was necessary to measure the effect of the cumulative cyclic loading on the stiffness of the motion segments. To the best of our knowledge there has only been one previous study examining the effect of repeated cycling on motion segment stiffness by Wilke *et al.* in 1998. This was performed in axial rotation on sheep spines, loaded to ±5Nm to a maximum of 500 loading cycles (Wilke et al., 1998a). It showed that there was no significant change in motion segment stiffness in axial rotation after 500 load cycles provided that temperature, loading rate and humidity were constant. Unfortunately this does not address the effect of cyclic loading on motion segment stiffness in the other two primary motion directions; flexion/extension and lateral bending. There is also wide variation in the literature regarding the number of cycles performed and from which load cycles the data were collected. This has included a single loading cycle (Panjabi et al., 1981, Riley et al., 2004, Wilke et al., 1997), three loading cycles (Takeuchi et al., 1999, Busscher et al., 2010), four loading cycles (Oda et al., 2002), five loading cycles (Shillington et al., 2011) and ten loading cycles (Linde et al., 1989). Without appreciating the effect these differences have on the segment stiffness in all three main axes of movement, it would be difficult to compare the data resulting from these studies.

2.5.3. Effect of Progressive Dissection of the Thoracic Motion Segment

The aim of *in vitro* biomechanical testing is to replicate *in vivo* conditions in a controlled environment. This allows researchers to standardise the testing protocol and minimise confounding variables, therefore allowing better study of the factor of interest. Different laboratories and researchers have performed biomechanical testing with different levels of motion segment dissection. Some studies

have removed the ribs entirely (Wilke et al., 1996, Wilke et al., 1997); others have removed the ribs and part of the spinous process (Puttlitz et al., 2007, Shillington et al., 2011); while a third group have left a segment of the ribs and the entire length of the spinous process intact (Panjabi et al., 1976, Panjabi et al., 1981). This has made it difficult to compare the results from these studies as well as the ability to use these results for *in vivo* studies and applications. Oda *et al.* (Oda et al., 2002, Oda et al., 1996) described the importance of the costovertebral joints in the thoracic spine functional unit stability in both human and canine cadaveric studies. However, in these studies sequential destabilising, anterior to posterior and posterior to anterior, was performed. The excision of the costovertebral joints was preceded by a total discectomy or a laminectomy with bilateral facetectomy, therefore it was not possible to establish the exact effect of removing the costovertebral joints alone.

2.5.4. Effect of Repeat Freeze-Thaw Cycles

In the process of biomechanical testing, test design and setup is of paramount importance. Long and repeated tests may require more than a single session. In these situations it is necessary to subject the motion segments to more than one freeze-thaw cycle during a complete testing program. Therefore, it was necessary to assess the effect this would have on the test results in order to design the main study minimising this effect on the results. A recent study by (Tan and Uppuganti, 2012) found that flexibility increased (reduced stiffness) with increasing numbers of freeze-thaw cycles in motion segments of a mature (elderly) human cadaver lumbar spine. This was tested with a moment of ±7.5Nm in all primary directions of flexion/extension, lateral bending and axial rotation with measurements taken at the fifth cycle. Hongo (Hongo et al., 2008) explored the effect of freeze thaw cycles on the biomechanics of porcine lumbar motion segments under an applied moment of ±5Nm with three freeze-thaw cycles; the authors found that after the initial freeze there was no significant change for subsequent freeze-thaw cycles. Their specimens were tested in the same three axes of movement with data collected from the fifth load cycle.

2.6. VERTEBRAL BODY STAPLING

2.6.1. BACKGROUND:

As indicated in Section 2.3, the principles of growth modulation have been applied to the spine. Based on the success of growth modulation in limb deformities using staples (Blount and Clarke, 1949), Nachlas and Borden reported in 1951 successful use of vertebral body staples to produce and treat an experimental scoliosis in canines (Nachlas and Borden, 1951). This was the first reported use of vertebral body staples in the literature. Smith used the same technique for anterior convex vertebral body stapling to treat scoliosis in humans (Smith et al., 1954). Unfortunately his results were disappointing, mainly due to patient selection and staple design. The patients had congenital scoliosis with severe curves and little growth potential left in the spine; some staples broke or became loose and the procedure failed to correct the curves. These issues have recently been addressed by Betz *et al*. (Betz et al., 2003), who used a C-shaped staple constructed from a shape memory alloy (**SMA**) called NITINOL, manufactured by Medtronic Sofamor Danek (Memphis TN, USA). This alloy has a special property in that when cooled they can be deformed but when heated up to a specific transitional temperature they return to their original shape (memory). It is made up of a nickel and titanium alloy, the percentage of each determines the transitional temperature. This transitional temperature is around 30 degrees for the SMA staples, according to the manufacturer, which means that when they reach body temperature they resume the 'C' shape. This shape memory property allows the surgeon to insert the staple, while cool, with the prongs parallel to minimise bony trauma and as they warm up to body temperature they resume their original shape creating an area of compression as well as a shape that will be difficult to dislodge.

The advent of **V**ideo **A**ssisted **T**horacoscopic **S**urgery (VATS) has provided an opportunity to perform vertebral body stapling in a minimally invasive manner reducing morbidity and recovery time (Sucato, 2003).

2.6.2. SURGICAL TECHNIQUE: (FIGURES 17 - 18)

Under general anaesthetic the patient is positioned in a lateral decubitus position with the convex side of the scoliosis upwards and the upper side arm flexed and abducted on a support gutter away from the operating field (Betz et al., 2003, Trobisch et al., 2011). The operating table is not flexed. Vertebral levels are checked with the image intensifier and intended portal sites marked on the skin. A double lumen endotracheal tube is used to deflate the upper side lung. Thoracoscopic portals are made in the intercostal spaces with the first between the 5^{th} and 7^{th} intercostal space. Usually 3-4 portals are needed. All levels involved in the Cobb angle measurement are stapled. A trial inserter is used to measure the width of the staple to be used and create pilot holes. This is confirmed with fluoroscopy. The desired staple is then prepared after being cooled over ice and the prongs are straightened using specific prong benders. The staple is inserted through the pilot holes. The process is repeated for all the involved levels. Care is taken to preserve the segmental vessels. A chest drain is inserted and the lung is reinflated. Final fluoroscopic images are taken. Post-operative use of a brace is debated between surgeons.

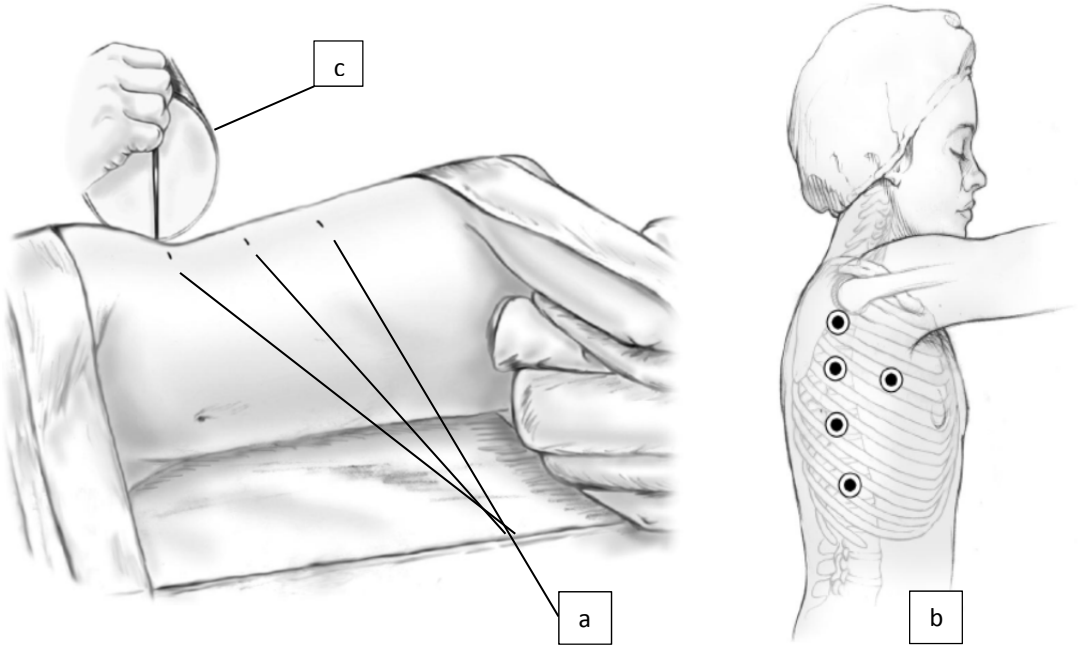

FIGURE 17: PATIENT POSITIONING AND PORTAL SITES FOR THORACOSCOPIC SURGERY (a, b) WITH RADIOLOGICAL ASSISTANCE USING FLEUROSCOPY (c) (BETZ ET AL., 2003).

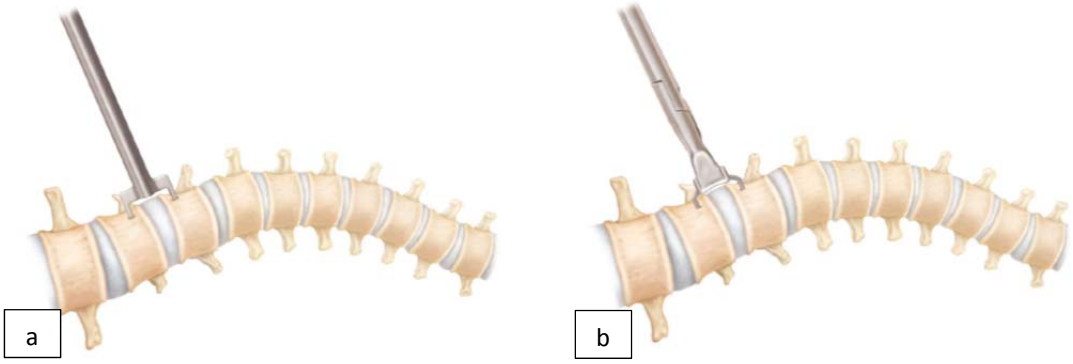

FIGURE 18: STAPLE INSERTION. a: SIZING THE INTERVERTEBRAL SPACE WITH TRIAL, b: INSERTION OF STAPLE (BETZ ET AL., 2003).

2.7. STAPLE DESIGN:

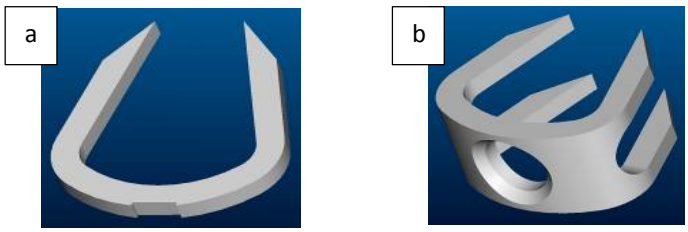

FIGURE 19: DIAGRAM OF a: 2 PRONG AND b: 4 PRONG SMA STAPLE (BETZ ET AL., 2003).

The SMA staples come in 2 shapes, 2 prongs and 4 prongs (Figure 19). The 4 prong design is the most commonly used in clinical practice. If the 2 prong staple is used 2 or 3 staples must be inserted at each level, whereas it's possible to use a single 4 prong staple at each level (Puttlitz et al., 2007, Betz et al., 2005). The upper and lower prongs are at a 30^{o} angle to an axis drawn perpendicular to the body of the staple. This angle can be straightened to 0^{o} (parallel) after cooling the staple, however, on reheating to $>30^{o}C$ it returns to its original shape (Figure 20). The prongs of the SMA staples are 2mm wide and 2.5mm thick proximal to the chamfer. They have a smooth surface. The 4 prong staples have an overall width of 10mm.

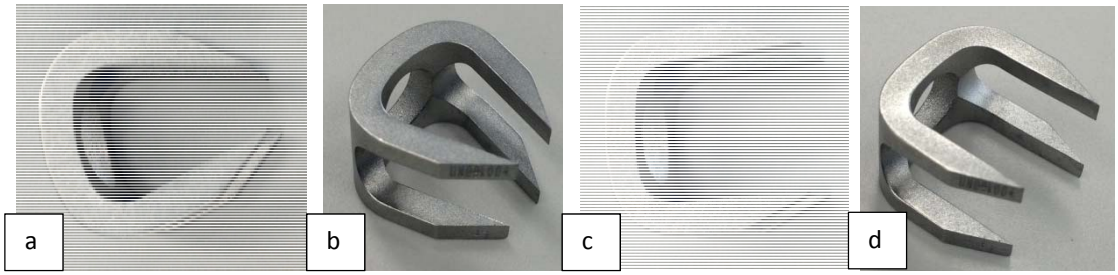

FIGURE 20: SMA STAPLE, a & b SHOW THE STAPLE IN ITS MEMORY SHAPE; c & d SHOW THE PRONGS STRAIGHTENED AFTER COOLING TO $0^{o}C$.

Recently, Medtronic Sofamor Danek has developed a prototype staple (Figure 21) made of titanium and incorporating a ratchet mechanism allowing 2mm of translation, to apply and maintain preload and compression. The prototype was included in this study. It is a 4 prong staple with prongs that are 2mm wide and 2.5mm thick. However, the prongs are barbed not smooth and are parallel.

FIGURE 21: PROTOTYPE STAPLE (a), IN OPEN POSITION (b) AND CLOSED (c)

3. MATERIALS AND METHODS

3.1. SPECIMENS:

Spines from twenty six 6-8 week old calves weighing 40-60kg were obtained from a local abattoir. Each had attached ribs and was frozen fresh on the day in double plastic bags at -20 degrees C. Each spine underwent a clinical CT scan to exclude congenital anomalies or injury.

3.2. SPECIMEN PREPARATION:

Each spine underwent the same thawing protocol (adopted from a previous study) (Thompson et al., 2004) as follows:

The spines were placed in a refrigerator (still double bagged) at 2^{o} C for 24 hrs. They were then taken out of the refrigerator and kept at room temperature (21 ^{o}C) for 4 hours during which they were dissected, with all attached musculature carefully removed, leaving the ligamentous attachments. The attached ribs were shortened to 5cm bilaterally. The spines were then divided into motion segments of T4-5, T6-7, T8-9 and T10-11, or T5-6, T7-8 and T9-10. Thus all motion segments from T4 to T11 were represented (Figure 22). Each study (Section 3.3) utilised two full sets of the seven motion segments (n=14). The choice of 14 segments per study was based on the prior work of Shillington *et al*. (Shillington et al., 2011), who found that a 10% change in the stiffness of immature bovine spinal segments could be detected with a power of 0.8 using n=14 specimens. Each segment consisted of two thoracic vertebral bodies, each with attached rib heads and 5cm of rib length, full length spinous processes and an intervertebral disc (Panjabi et al., 1981). Screws were inserted into the superior and inferior end plates to improve fixation in the polymethylmethacrylate into which they were potted. The segments were wrapped loosely in gauze and sprayed regularly with warmed (37 ^{o}C) buffered saline 0.9% and kept in the environment chamber at 37^{o}C for 1 hour (this was shown to raise the temperature of the intervertebral disc to 34^{o}C). The humidity was kept at 100% with regular spraying of the specimens with the buffered saline solution every 5 minutes.

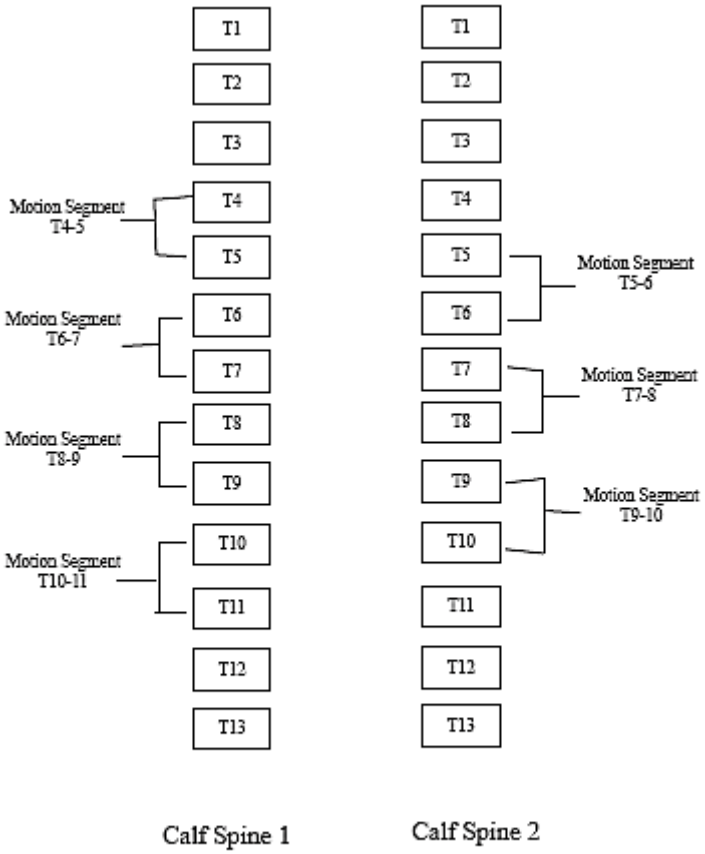

FIGURE 22: SCHEMATIC INDICATING THE MOTION SEGMENTS USED IN THIS STUDY. AS SHOWN IN THE SCHEMATIC TWO SPINE SPECIMENS WERE REQUIRED TO REPRESENT A SINGLE FULL T4 – T11 SPINE.

The potted segments were mounted onto a custom made testing jig which allowed free x-y (horizontal plane) movement with high precision linear bearings at the base (Figure 23). This design did not allow axial loading in flexion/extension or lateral bending. The axial load during axial rotation was kept bellow ±0.1N. Testing was performed using an Instron Biaxial Testing Machine (Instron, 8874, Norwood, Massachusetts, USA) which has a load capacity of ±10 kN with an accuracy of ±0.05N and a torque capacity of 100Nm and a measurement accuracy of within ±0.005Nm. It uses a biaxial Instron Dynacell transducer measuring force and torque. Each test was performed in the sequence of flexion/extension followed by lateral bending and finally axial rotation. Data sampling was at the rate of 100Hz. The force required to overcome static friction in the x-y bearing plate was measured to be 0.49N. This resulted in a frictional moment of 0.12Nm in the flexion/extension and lateral bending modes. In axial rotation the frictional moment was negligible due to the plate being mounted on the loading axis of the testing machine for these tests.

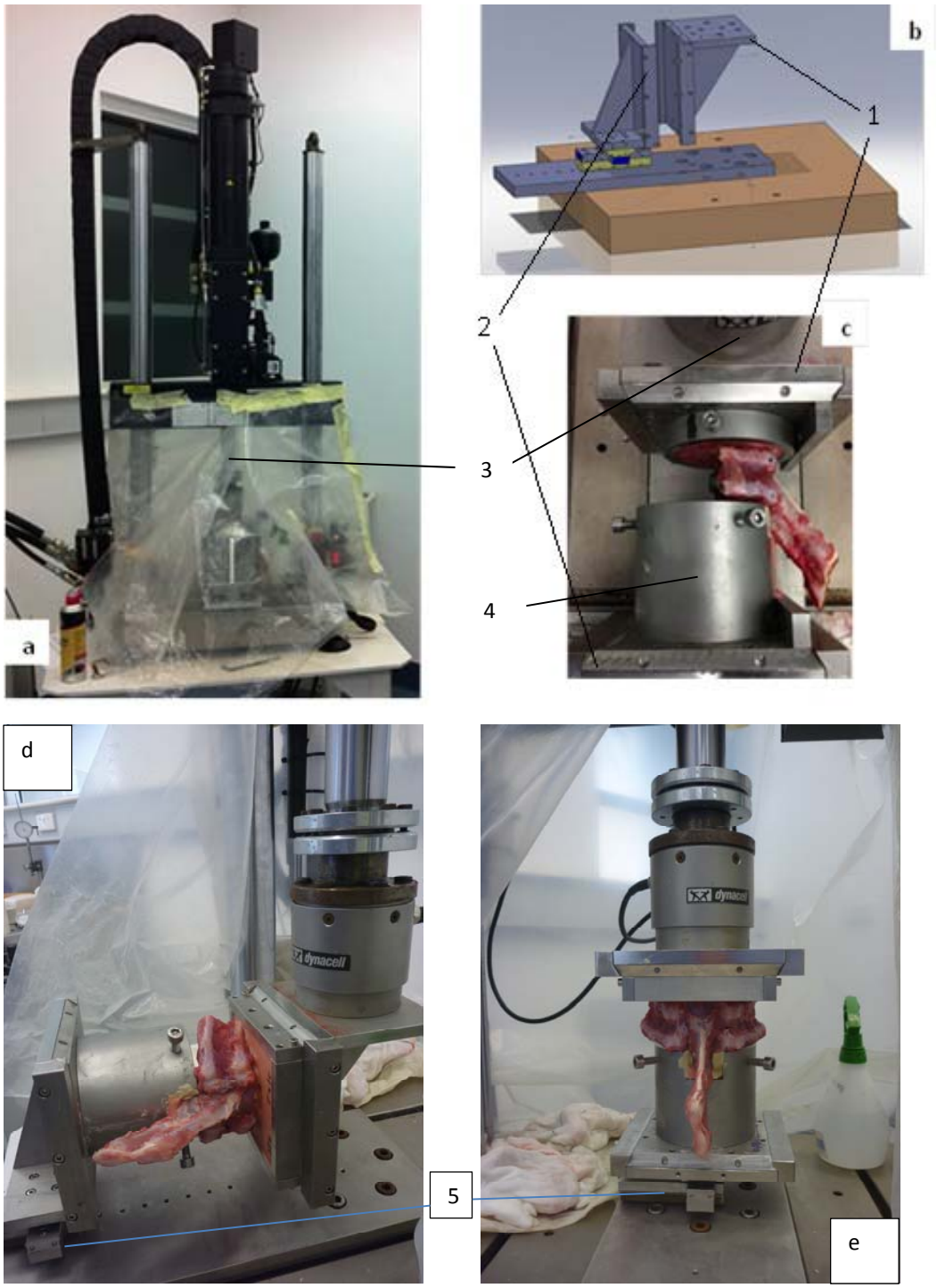

FIGURE 23: a) INSTRON BIAXIAL MATERIALS TESTING MACHINE, b) CUSTOM MADE TESTING JIG WITH FREE HORIZONTAL PLANE MOVEMENT. THE DIAGRAM SHOWS THE JIG SET UP FOR FLEXION/EXTENSION AS PLATE (1) ATTACHES TO THE VERTICAL TESTING SHAFT OF THE INSTRON AND THE OTHER PLATE (2) ATTACHES TO THE CAUDAL ANCHORING PLATE ON THE FREE X-Y MOVEMENT JIG, c) EXAMPLE OF TEST SPECIMEN IN JIG SET UP TO TEST FLEXION/EXTENSION, (3) REPRESENTS THE VERTICAL INSTRON TESTING SHAFT WHICH ROTATES TO PROVIDE FLEXION/EXTENSION, (4) SHOWS AN EXTENSION TUBE USED TO ALLOW CLEARANCE OF THE SPINOUS PROCESS. d) SHOWS THE TESTING JIG SET UP FOR FLEXION/EXTENSION, e) SHOWS THE JIG SET UP FOR AXIAL ROTATION. (5) HIGH PRECISION BEARINGS.

3.3. STUDY DESIGN

The studies were divided into 2 groups (see Table 1 below):

1. Pilot studies (I-IV) to validate the testing model, assess the effect of confounding variables and design the main studies.
2. Main studies to examine the effect of staple insertion on the biomechanics and structure of the motion segments.

Study Name	**Objective**		**Calf Spine ID Number**	**Number of segments used**
Pilot I	Define moment required in each axis to achieve the desired range of motion		2, 6, 8 and 10	14 (2xT4-5, 2xT5-6, 2xT6-7, 2xT7-8, 2xT8-9, 2x T9-10, 2xT10-11)
Pilot II	Assess the effect of cumulative cyclic loading and define the "N^{th}" cycle		9, 14, 15 and 18	14
Pilot III	Assess the effect of progressive dissection		1, 22, 26 and 27	14
Pilot IV	Assess the effect of multiple freeze thaw cycles		2, 4, 5 and 7	14
Main Study I	Assess the effect of staple insertion on segment stiffness	SMA Staple	19, 11, 21 and 23	14
		Prototype Staple	3, 12, 17 and 20	14
Main Study II	Assess the effect of staple insertion on the vertebral bone structure	SMA Staple	19, 11, 21 and 23	14 (from Main Study I)
		Prototype Staple	3, 12, 17 and 20	14 (from Main Study I)
Main Study III	Assess the effect of staple insertion and single axis movement on the stiffness and vertebral bone structure	SMA Staple	24	3 (1x 5/6, 1x7/8, 1x9/10)
		Prototype	25	3 (1x 5/6, 1x7/8, 1x9/10)

TABLE 1: STUDY DESIGN AND SEGMENTS USED IN EACH STEP. "N" IS THE NUMBER OF CYCLES USED IN SUBSEQUENT TESTS

3.3.1. Pilot Study I: Load magnitude

This study was performed to determine the moment necessary to achieve 6 degrees of rotation in each direction for all three main axes (flexion/extension, lateral bending and axial rotation). It was also used to study the type of statistical distribution of the specimens.

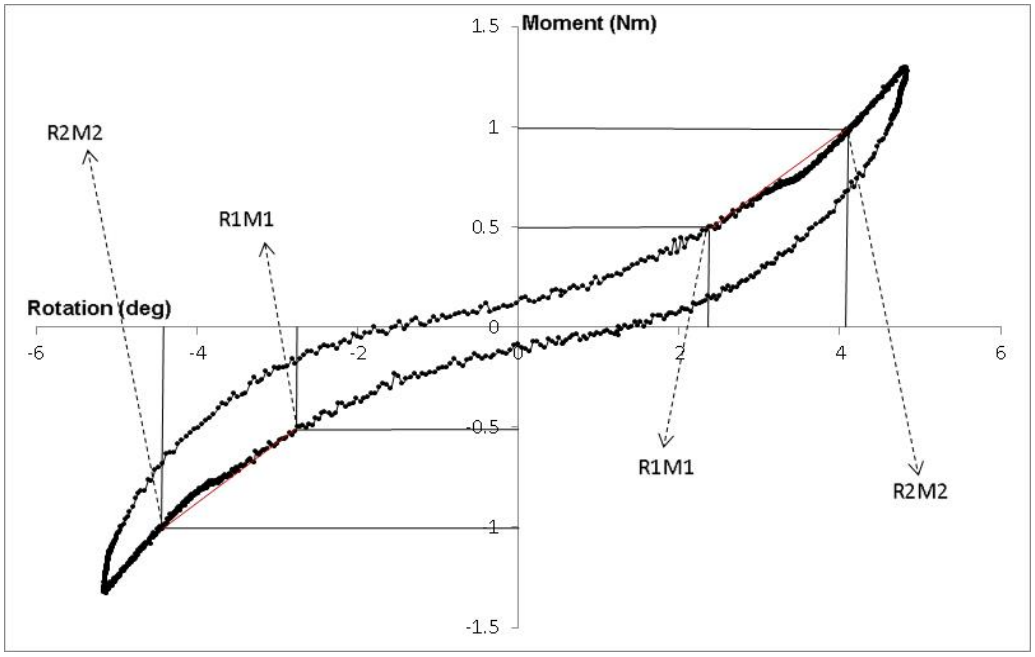

FIGURE 24: TYPICAL MOMENT VS. ROTATION CURVE INDICATING POINTS FOR STIFFNESS CALCULATION. R1M1= ROTATION 1, MOMENT 1; R2M2= ROTATION 2, MOMENT 2. THE CURVE SHOWS BOTH POSITIVE MOMENT APPLICATION (FLEXION, RIGHT LATERAL BENDING OR RIGHT AXIAL ROTATION) AND NEGATIVE MOMENT APPLICATION (EXTENSION, LEFT LATERAL BENDING OR LEFT AXIAL ROTATION).

The potted specimens were mounted on the custom made jig and tested using displacement control with continuous ramping for 10 load cycles in each axis to ±6 degrees at a rate of 1 degree per second, with a cut off abort moment of 4Nm. Data for moment and rotation from the 10th load cycle were collected for analysis. The mean maximum moments for each axis (M_{fe}, M_{lb}, M_{ar}) were then applied for moment-controlled loading in subsequent studies. Analysis of the moment vs rotation curves was used to determine the points for measuring the segment stiffness (Figure 24). Stiffness was calculated from the moment vs. rotation curve between 0.5 Nm and 1 Nm using the equation: Stiffness = (Moment2-Moment1)/(Rotation2-Rotation1).

3.3.2. Pilot Study II: Effect of cumulative cyclic loading

This study was designed to assess the effect of cumulative cyclic loading on the motion segment stiffness. The potted segments were tested under moment control to ±M (Nm) at a rate of 0.3Nm per second with a cut off abort rotation of 10 degrees, for 500 continuous load cycles in each axis of movement. Data were collected from cycles 3, 5, 10, 25, 100, 200, 300, 400 and 500. Moment vs rotation data were used to determine stiffness of the segments. Analysis of the data collected from this study determined the number of load cycles "N" to be used in subsequent studies. This was determined as the data collection point with the least cumulative loading effect on motion segment stiffness; as each segment will be required to undergo 3 x "N" number of load cycles for each test phase.

3.3.3. Pilot Study III: Effect of progressive dissection

This study was designed to assess the effect of progressive dissection on the motion segment stiffness, specifically, the excision of the ribs and spinous processes.

The potted motion segments were tested under moment control to ±M (Nm) at a rate of 0.3Nm per second with a cut off abort rotation of 10 degrees, for N cycles of continuous cyclic loading. The data were collected from the N^{th} cycle. Next the ribs were excised and the testing was repeated. Finally the spinous processes were excised at their base, keeping the laminae intact, and the testing was repeated again. Moment vs rotation data were used to determine segment stiffness.

3.3.4. Pilot Study IV: Effect of multiple freeze-thaw cycles

This study was designed to assess the effect of multiple freeze-thaw cycles on the motion segment stiffness. The potted specimens were tested under moment control to ±M (Nm) at a rate of 0.3Nm per second with a cut off abort rotation of 10 degrees, for N cycles of continuous cyclic loading. The specimens were then refrozen for 48 hours and re-thawed with the same protocol. The segments were then tested as before. This was repeated for a total of five freeze-thaw cycles. The collected moment vs rotation data were used to measure segment stiffness.

3.3.5. Main Study I: Effect of staples on motion segment stiffness

This study was designed to assess the effect of vertebral body staple insertion on the stiffness of the motion segments. Two types of staples were used. Both manufactured by Medtronic Sofamor Danek. One was the **S**hape **M**emory **A**lloy (SMA) staple and the other was a titanium Ratcheting Staple (Prototype) (Figure 25).

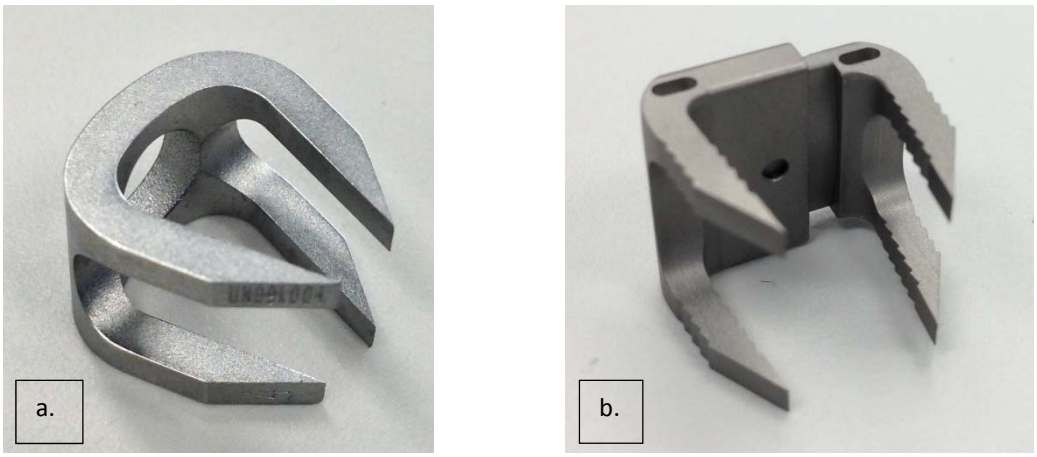

FIGURE 255: VERTEBRAL BODY STAPLES. a. SHAPE MEMORY ALLOY (SMA), b. RATCHETING PROTOTYPE STAPLE.

The potted specimens were first tested un-instrumented to moment ±M (Nm) at a rate of 0.3Nm per second with a cut off abort rotation of 10 degrees, for N cycles of continuous cyclic loading. Next a left anterolateral staple was inserted with the testing jig locked with a bridging brace to protect the specimen. The brace was removed and the segment was then tested again using the same protocol. Each staple type was tested on fourteen motion segments. The collected moment vs rotation data were used to calculate segment stiffness (Figure 24).

3.3.6. Main Study II: Vertebral bone damage due to staple insertion

This study was designed to assess the effect of staple insertion and cyclic loading on the bony structure of the motion segments.

After testing, the motion segments from the previous study had the staples carefully cut with a diamond saw, to allow the removal of the staple prongs without creating any additional trabecular

damage, and carefully removed with fine pliers. The ribs were excised and the neural arch removed. The specimens were then fixed in 100% Ethanol and Micro **C**omputed **T**omography scanning of each motion segment was performed. The Micro CT scans were analysed using ImageJ where they were reconstructed into axial, sagittal and coronal slices to allow the measurement of the maximum length, width and thickness of the tracks created by the staple prongs. These were measured using ImageJ. However there was great variability in the insertion length of the prongs. This was a result of the insertion technique and positioning of the staple. To overcome this variability the cross section of the prong just proximal to the chamfer was used for analysis. Cross section measurements were then analysed against the collected stiffness data for these segments.

The data were also used to classify the staple insertions into three grades depending on the number of epiphyseal plates (superior and inferior) damaged by the staple prongs. Segments with neither plate affected were assigned a grade 0, those with one plate affected grade 1 and when both plates were affected grade 2.

3.3.7. Main Study III: Assess the effect of staple insertion and *single axis* movement on motion segment stiffness and vertebral bone structure

This study was performed to assess the effect of movement of the staple in the vertebral bodies during testing on motion segment stiffness after staple insertion for each axis as well as the bone damage from this movement. Six segments (three for the SMA staple and three for the prototype) were prepared as in the previous studies.

The potted specimens were first tested un-instrumented to moment ±M (Nm) in one axis only (flexion/extension, lateral bending or axial rotation) at a rate of 0.3Nm per second with a cut off abort rotation of 10 degrees, for N cycles of continuous cyclic loading. Next a left anterolateral staple was inserted with the testing jig locked with a bridging brace to protect the specimen. The brace was removed and the segment was then tested again in the same axis using the same protocol. The collected moment vs displacement data were used to measure segment stiffness according to the technique outlined in Section 3.3.1.

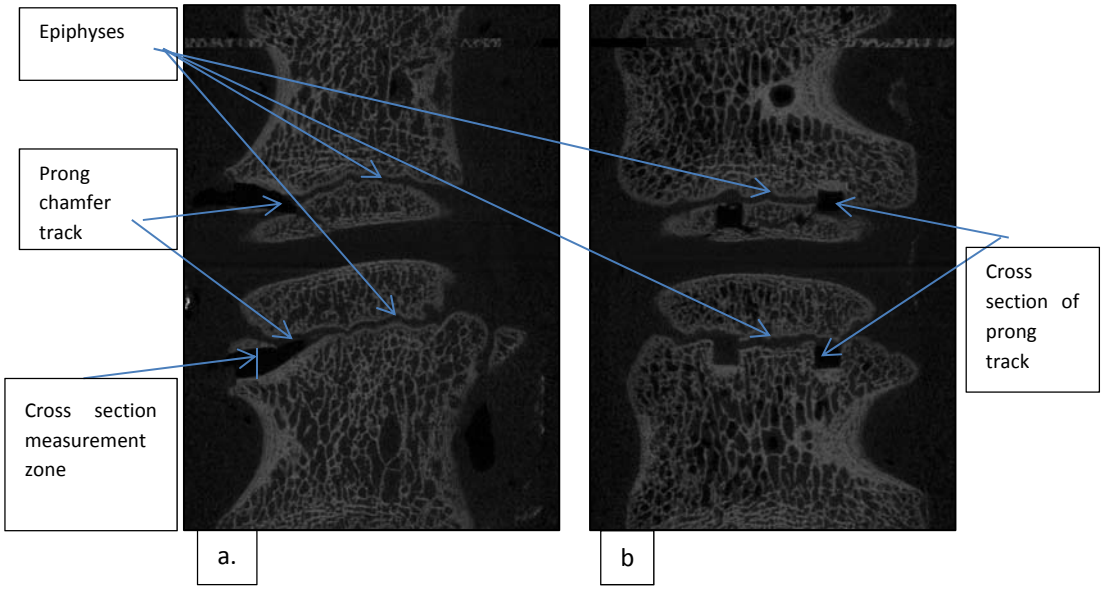

FIGURE 26: EXAMPLE OF MICRO CT OF A MOTION SEGMENT SHOWING EPIPHYSES AND STAPLE PRONG TRACKS. a. LONGUTUDINAL SECTION THROUGH PRONG TRACK. b. CROSS SECTION THROUGH PRONG TRACK AT THE MEASUREMENT ZONE.

Next the staples were cut with a diamond saw in order to allow removal without causing further damage to the surrounding bone, and carefully extracted using fine pliers. The ribs were excised and the neural arch removed. The specimens were then fixed in 100% Ethanol and underwent Micro CT scanning. Data files from the Micro CT were analysed using ImageJ where the images were reconstructed into axial, sagittal and coronal slices to measure the maximum length (L), width (W) and thickness (D) of the tracks created by the staple prongs (Figure 26). These were measured using ImageJ. The cross sections of the prongs just proximal to the chamfer were measured and were then analysed against the collected stiffness data for these segments.

3.4. STATISTICAL ANALYSIS

Stiffness was calculated from the moment vs. rotation curve between ±0.5 Nm and ±1Nm according to: Stiffness = (Moment2-Moment1)/(Rotation2-Rotation1). Mean, standard deviation, median, mode, standard error of mean, minimum and maximum stiffness were calculated for each data collection cycle. Data from each group were tested for normality using the Kolmogorov-Smirnov test. Statistical analyses of the data were performed using SPSS (version 21.0, IBM, Armonk, NY) generalised linear models for repeated measures, ANOVA with pairwise testing using Bonferroni correction and T-tests. A significance level of $P<0.05$ was considered statistically significant. For each test, motion segment stiffness (k) was normalised to the initial value (ko) to allow graphing of changes in stiffness ratio (k/ko) over the course of testing.

4. RESULTS:

4.1. BIOMECHANICAL PROPERTIES OF IMMATURE BOVINE SPINE MODEL:

The mean torque required to achieve 6 degrees of rotation during flexion/extension was 1.73Nm, for lateral bending it was 1.05Nm and for axial rotation it was 1.27Nm (Figure 27). The maximum torque (Table 2) for flexion/extension was 2.45Nm, for lateral bending was 1.78Nm and for axial rotation was 2.09Nm.

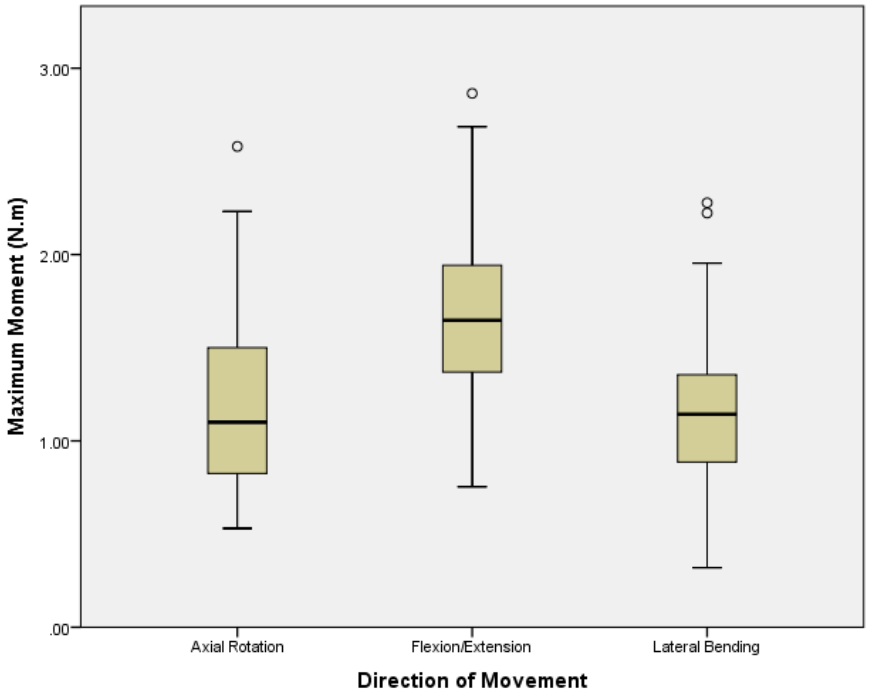

FIGURE 27: BOXPLOT OF THE TORQUE REQUIRED IN EACH DIRECTION OF MOVEMENT.

The specimens followed a normal distribution using the Kolmogorov-Smirnov test in each direction of movement.

Direction of Movement	Mean Moment (N.m)	Minimum Moment (N.m)	Maximum Moment (N.m)	Standard Error (N.m)
Flexion/Extension	1.73	1.25	2.45	0.086
Lateral Bending	1.05	0.35	1.78	0.114
Axial Rotation	1.27	0.69	2.09	0.1

TABLE 2: PILOT STUDY RESULTS USED TO DETERMINE MOMENT IN EACH PLANE OF MOTION REQUIRED TO ACHIEVE APPROXIMATELY ±6 DEGREES OF ROTATION FOR SUBSEQUENT TESTS.

4.2. THE EFFECT OF PROGRESSIVE CYCLIC LOADING:

The effect of cumulative cyclic loading was initially tested as the first data point (3rd cycle) and the last data point (500th cycle). After this each data point was compared to the remaining nine other data points using Bonferroni correction to identify the point at which the difference becomes significant.

In flexion/extension (figure 28a), there was a 22% decrease in stiffness from the initial (3^{rd} cycle) stiffness of 0.39 $Nm.deg^{-1}$ over 500 cycles of loading. This was a significant difference with P=0.001. Further pairwise tests showed that a statistically significant difference was only evident after the 50^{th} cycle. However using the 5^{th} cycle (rather than the 3^{rd}) as a baseline increased the number of cycles needed to produce a significant effect to the 200^{th} cycle. On further analysis of flexion vs extension, the decrease in stiffness with increasing number of cycles was equally apparent in both flexion and extension as shown in Figure 29d.

In right and left lateral bending (Figure 28b) there was an 18% decrease in stiffness over 500 cycles of loading, compared to the initial (3^{rd} cycle) value of 0.31 $Nm.deg^{-1}$. This was significant, P=0.009. Pairwise tests showed this decrease to be insignificant up to the 400^{th} cycle, after which there is an 8% drop in stiffness between the 400^{th} and 500^{th} cycles; this made the overall stiffness change become statistically significant. In contrast to the

statistically significant change in flexion/extension stiffness between the 5th and 200th cycles, the 5% drop in lateral bending stiffness between these cycles was not statistically significant.

In right and left axial rotation there was no significant change in motion segment stiffness with the increasing number of load cycles (Figure 28c). From the initial (3rd cycle) stiffness value of 0.29Nm.deg^{-1} there was a total increase of 9% in the mean motion segment stiffness over 500 load cycles, however this was not statistically significant, P=0.137. Pairwise tests were insignificant. Also, in contrast to the statistically significant change in flexion/extension stiffness between the 5th and 200th cycles, the 6% increase in axial rotation stiffness between these cycles was not statistically significant.

From this study the Nth cycle was calculated to be the 10th cycle for use in subsequent tests.

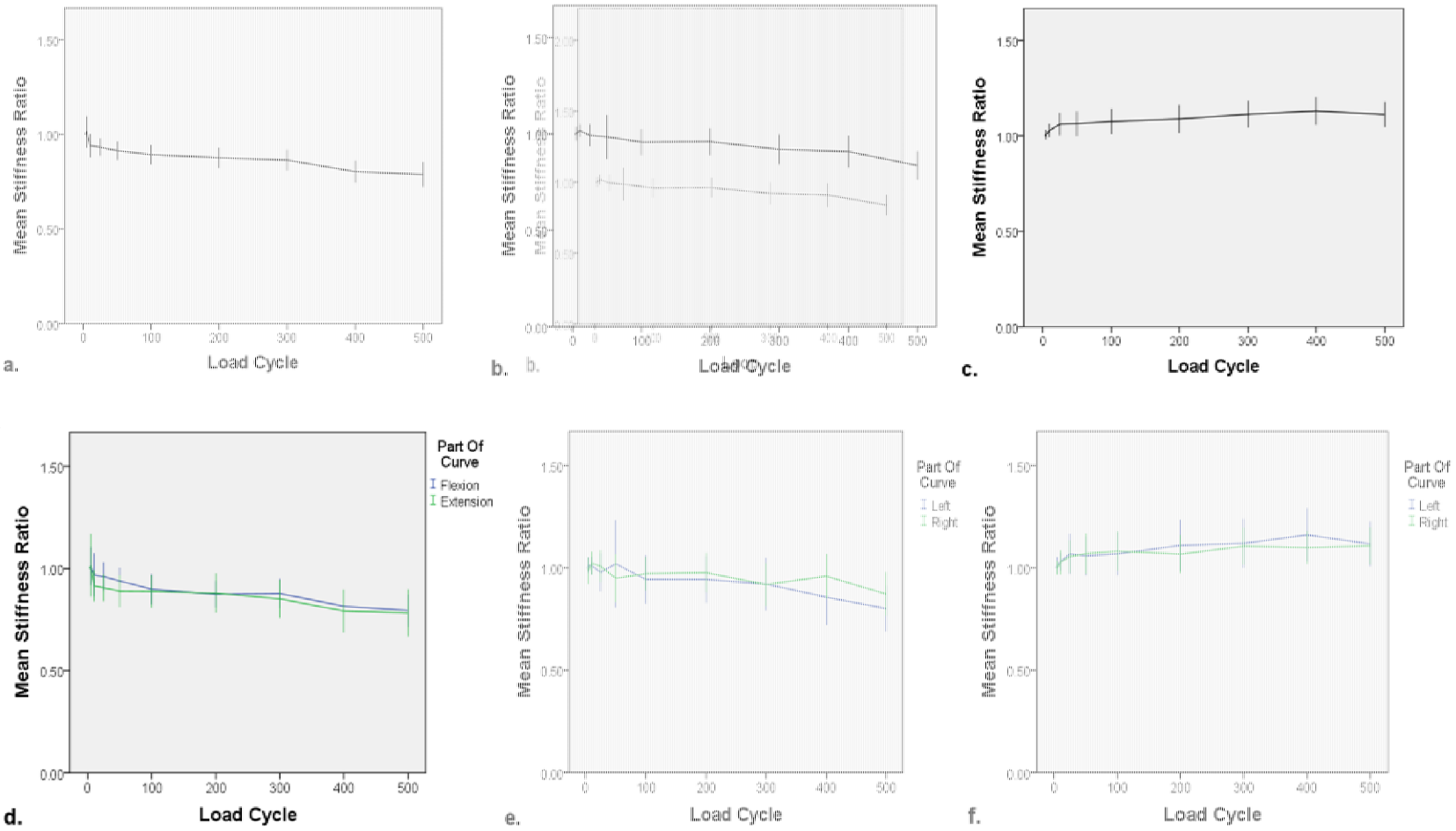

FIGURE 28: MEAN STIFFNESS RATIOS* (K/K0) VS. LOAD CYCLE NUMBER. a: FLEXION/EXTENSION, b: LATERAL BENDING, c: AXIAL ROTATION. d: DEMONSTRATING FLEXION AND EXTENSION SEPARATELY, e: DEMONSTRATING LEFT AND RIGHT LATERAL BENDING INDIVIDUALLY AND f: DEMONSTRATING LEFT AND RIGHT AXIAL ROTATION SEPARATELY. ERROR BARS INDICATE 95% CONFIDENCE INTERVAL. K0 IS TAKEN FROM THE 3RD LOAD CYCLE.

4.3. THE EFFECT OF PROGRESSIVE DISSECTION OF THE THORACIC FSU:

In flexion/extension (Figure 29a), there was an 18% reduction in stiffness of the motion segment, from the initial value of 0.37Nm.deg^{-1} after removing the ribs and spinous process, which was significant *P*=0.043. The significant drop occurred after resection of the rib heads with a reduction in stiffness of 18%, *P*=0.036. This significance was expressed mainly in flexion (Figure 29d) with a reduction in stiffness of 22%, *P*=0.05. This was in contrast to extension, in which stiffness dropped by 13% only, *P*=0.478. However, there was no further significant change in stiffness on resection of the spinous process in either flexion or extension (<1%), *P*=1.00.

In lateral bending (Figure 29b), there was a decrease in stiffness from the initial value of 0.33Nm.deg$^{-1,}$ of 18% which was significant *P*=0.023. Of this drop 13% occurred after resection of the ribs, however, this alone was not statistically significant (*P*=0.184). There was no difference between left and right curves (Figure 29e).

In axial rotation (Figure 29c), from the initial value of 0.38 Nm.deg^{-1}, there was a decrease of stiffness of 6.5%; however, this was not significant *P*=0.253. There was no difference between left and right curves (Figure 29f).

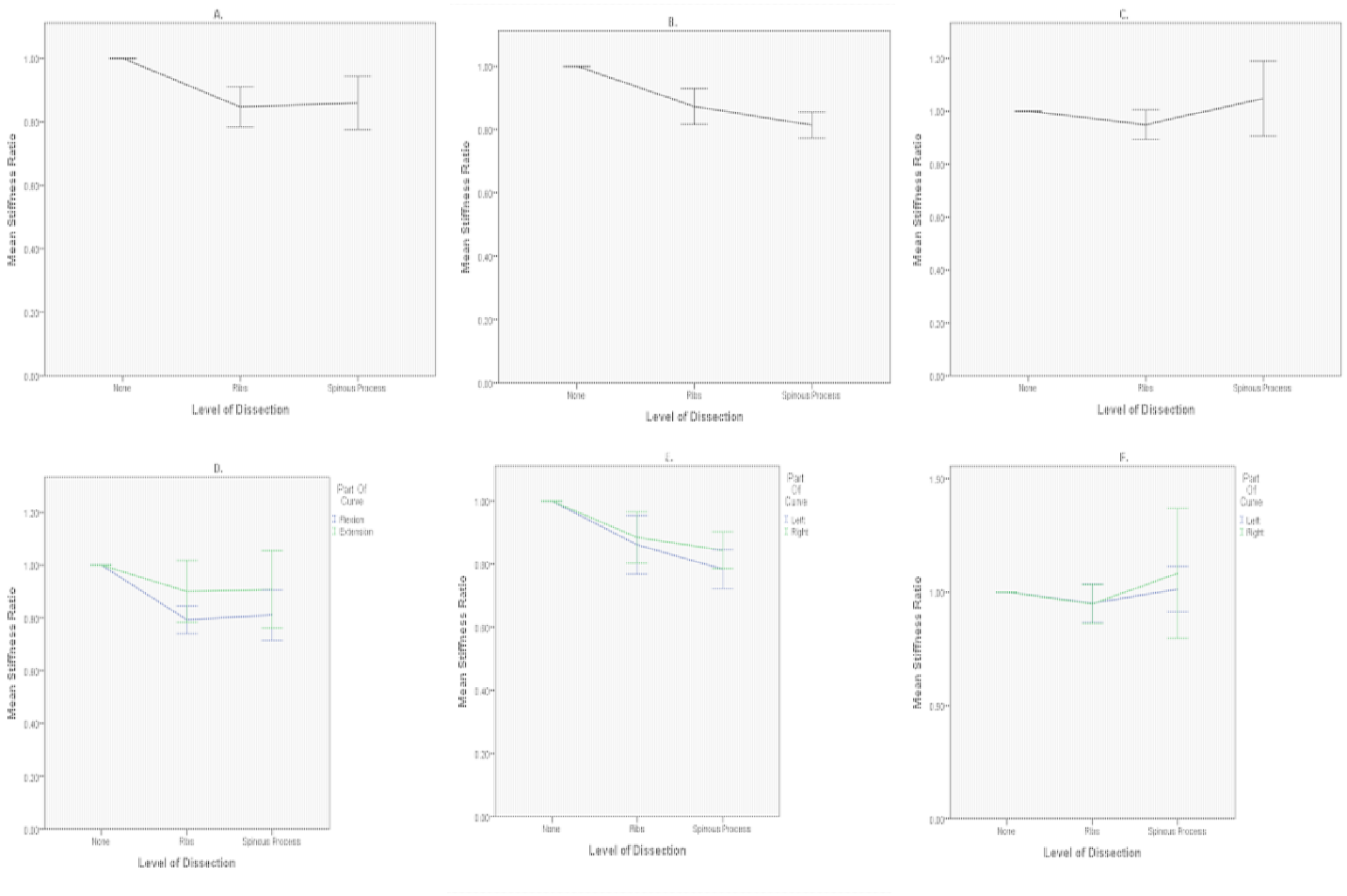

FIGURE 29: MEAN STIFFNESS RATIOS* (K/K0) VS. LEVEL OF DISSECTION. a: FLEXION/EXTENSION, b: LATERAL BENDING, c: AXIAL ROTATION. d: DEMONSTRATING FLEXION AND EXTENSION SEPARATELY, e: DEMONSTRATING LEFT AND RIGHT LATERAL BENDING INDIVIDUALLY AND f: DEMONSTRATING LEFT AND RIGHT AXIAL ROTATION SEPARATELY. ERROR BARS INDICATE 95% CONFIDENCE INTERVAL. K0 IS TAKEN FROM THE SPINE SEGMENT STIFFNESS PRIOR TO ANY EXCISIONS.

4.4. THE EFFECT OF REPEAT FREEZE-THAW CYCLES:

In flexion/extension (Figure 30a), there was no significant change in motion segment stiffness between freeze-thaw cycles one and five from the initial stiffness value of 0.27 $Nm.deg^{-1}$ (*P*=0.813). However, on further analysis of the individual effects on flexion and extension (Figure 30d), there was no significant change in flexion stiffness (*P*=0.336) but a significant (*P*=0.041) 9% decrease in extension stiffness; as the graph shows there was an initial (non-significant) increase in extension stiffness between the 1st and 2nd freeze cycles of 23% (*P*=0.114).

In lateral bending, as shown in Figure 31b, there was a statistically significant increase in motion segment stiffness in lateral bending from the initial value of 0.2 $Nm.deg^{-1}$, with repeated freeze-thaw cycles, of 26% (*P*=0.003). There was no statistically significant difference between left and right lateral bending stiffness (*P*= 0.598) (Figure 30e). However between the 1st and 2nd freeze cycles there was a 20% increase in stiffness which was near significant (*P*=0.088). This was followed by a transient drop in stiffness of 5% over the 3rd and 4th freeze/thaw cycles, followed by a 10% increase. Neither of these changes was statistically significant.

In axial rotation (Figure 30c), there was no statistically significant change in motion segment stiffness with repeated freeze-thaw cycles; however the *P*-value of 0.07 was near-significant, with a mean reduction in motion segment stiffness of 6% relative to the initial value of 0.28 $Nm.deg^{-1}$. The largest reduction occurred between the 1st and 2nd freeze cycles of 9% which was statistically significant (*P*= 0.04). Following this there was a mild increase in segment stiffness over the subsequent freeze/thaw cycles of 4% which was not statistically significant. There was no statistically significant difference between left and right axial rotation (*P*=0.111).

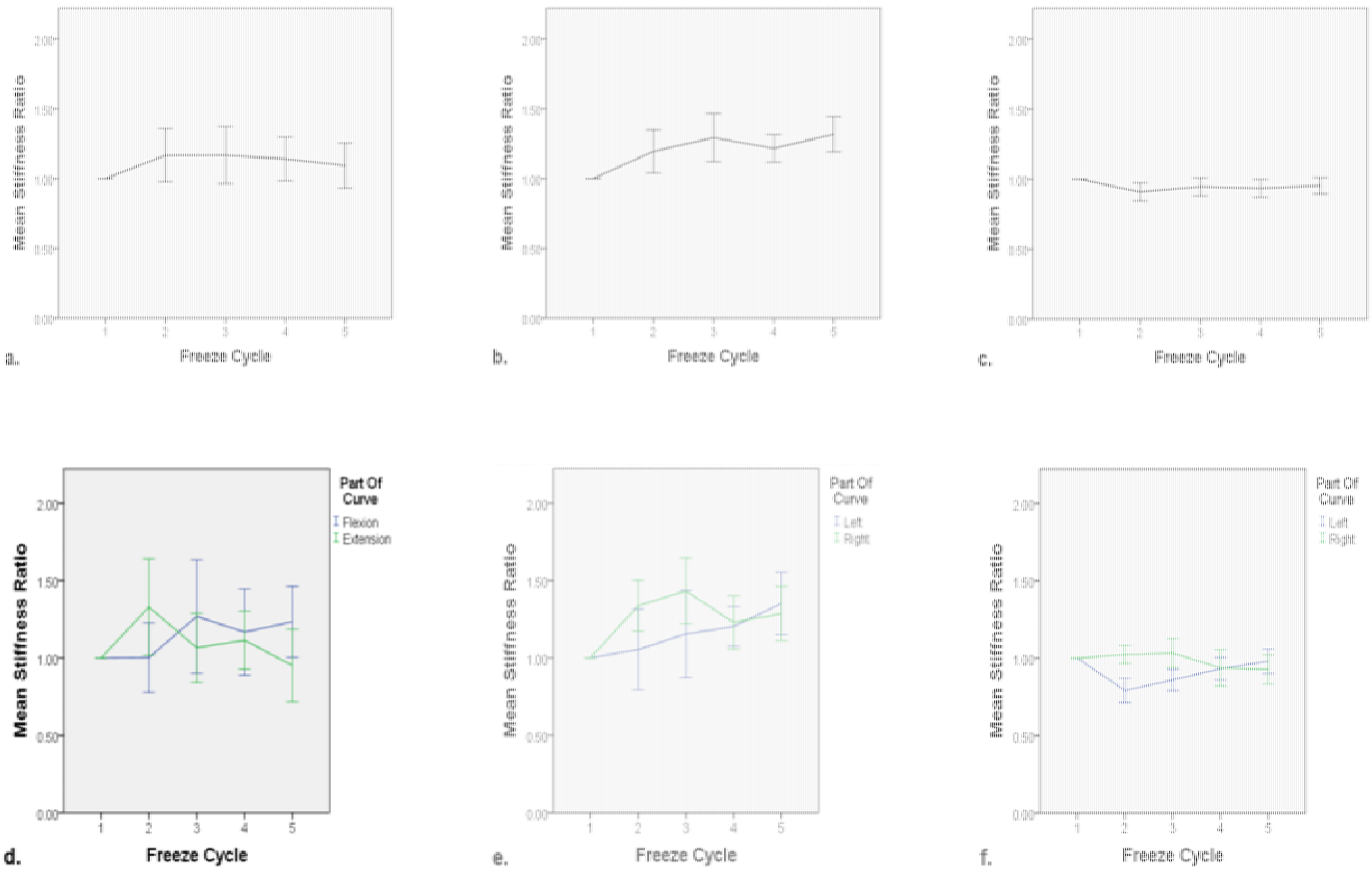

FIGURE 30: MEAN STIFFNESS RATIOS (K/K0) RELATIVE TO FREEZE-THAW CYCLE NUMBER. a. FLEXION, EXTENSION, b. LATERAL BENDING, c. AXIAL ROTATION, d. DEMONSTRATING FLEXION AND EXTENSION SEPARATELY, e. DEMONSTRATING LEFT AND RIGHT LATERAL BENDING SEPARATELY, f. DEMONSTRATING RIGHT AND LEFT AXIAL ROTATION SEPARATELY. ERROR BARS INDICATE 95% CONFIDENCE INTERVAL. K0 IS TAKEN FROM THE FIRST FREEZE-THAW CYCLE.

4.5. THE EFFECT OF VERTEBRAL BODY STAPLE INSERTION:

4.5.1. THE SHAPE MEMORY ALLOY (SMA) STAPLE:

In flexion/extension there was a drop in motion segment stiffness of 3% from 0.30Nm.deg^{-1} after staple insertion (Figure 31a). This was statistically insignificant (P=0.478) and was equally observed in both flexion and extension.

In lateral bending (Figure 31b), there was a significant drop in stiffness of 21% from 0.30Nm.deg^{-1} after staple insertion (P<0.001). This was observed mainly in lateral bending to the right (away from the staple), where the stiffness decreased by 30% (P<0.001). This was in contrast to lateral bending to the left (towards the staple) where it dropped by only 12% which was still statistically significant (P=0.036).

In axial rotation (Figure 31c), there was an overall near significant drop in stiffness of 11% (P=0.076) from the initial stiffness of 0.27Nm.deg^{-1} after staple insertion. However this was more to the left (towards the side of the staple), measuring a decrease of 14% as opposed to 8% to the right (away from the staple). In both directions it was a statistically insignificant drop (P=0.134 and P=0.352 respectively).

Further analysis comparing the motion segment stiffness in the second load cycle with that of the tenth revealed no significant change in stiffness in all 3 axes of movement (flexion/extension P= 0.300, lateral bending P= 0.914, axial rotation P= 0.093) as shown in Figure 31d, e and f..

4.5.2. THE PROTOTYPE STAPLE:

In flexion/extension (Figure 31a), there was a significant drop of 10% (P=0.004) from the pre-insertion stiffness value of 0.40Nm.deg^{-1}. This was observed in both flexion 10% (P= 0.062) and extension 10% (P= 0.036).

In lateral bending (Figure 31b), there was a statistically significant drop in stiffness of 9% (P=0.023) on staple insertion from 0.35Nm.deg^{-1}. Unlike the SMA staple this was more toward the staple with a reduction in stiffness of 14% (P=0.001), than away from the staple where it was reduced by 4% (P=0.594).

In axial rotation (Figure 31c), unlike the SMA staple, there was a significant reduction in stiffness of 13% (P<0.001) from 0.32Nm.deg^{-1} with staple insertion. This was slightly more away from the staple 14% (P= 0.010) than towards the staple where it was reduced by 12.5% (P=0.005).

Further analysis comparing the motion segment stiffness in the second load cycle with that of the tenth (Figure 31d), revealed no significant change in stiffness in flexion/extension (P=0.415). However, there was a significant change in lateral bending stiffness with an increase of 4% (P=0.040) (Figure 31e) and in axial rotation there was an increase of 8% (P=0.005) between the 2nd and 10th load cycles (Figure 31f).

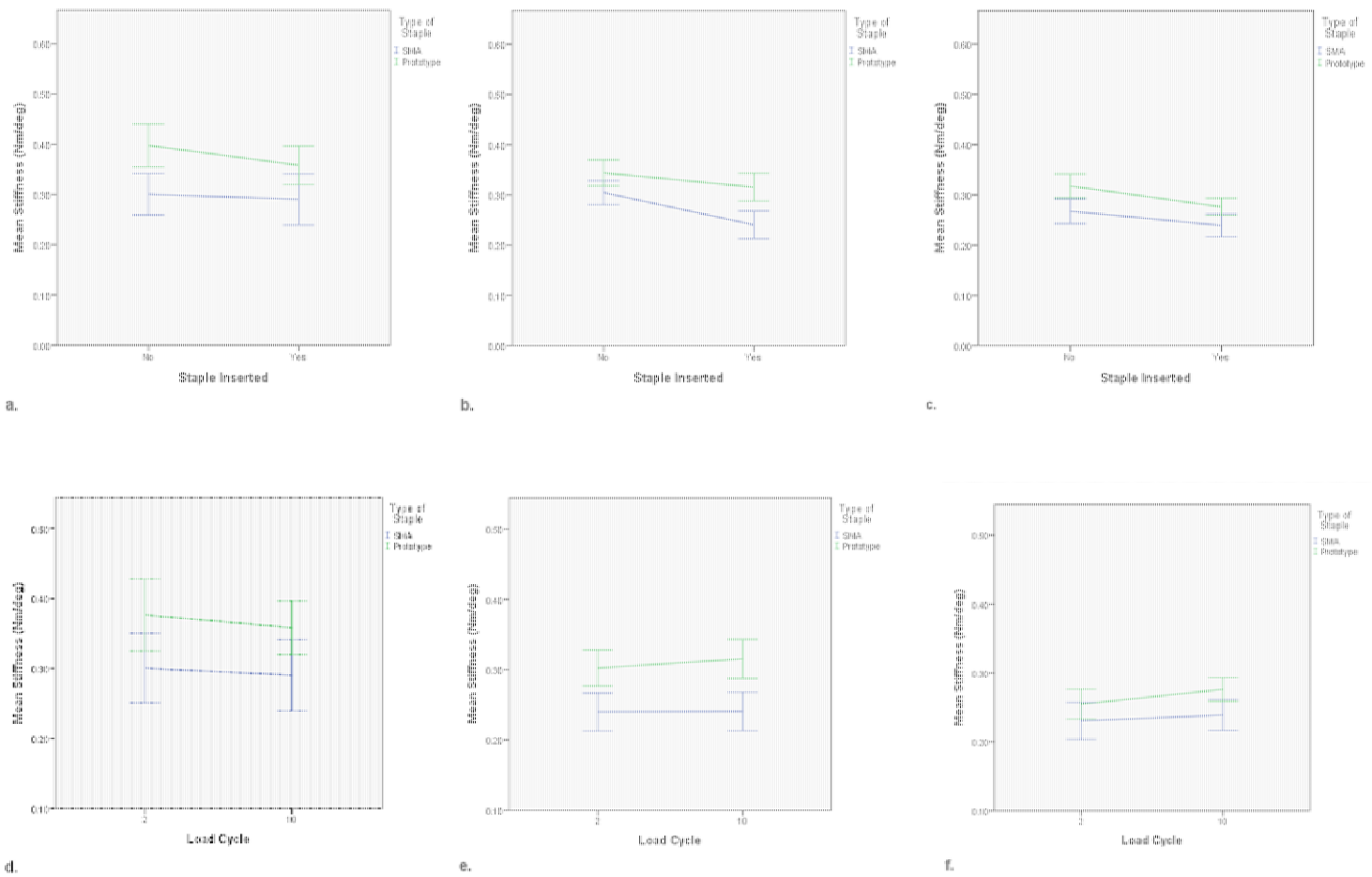

FIGURE 31: THE EFFECT OF SMA AND PROTOTYPE STAPLES ON MOTION SEGMENT STIFFNESS. a. FLEXION/EXTENSION, b. LATERAL BENDING, c. AXIAL ROTATION. d., e. AND f. SHOW THE CHANGE IN SEGMENT STIFFNESS BETWEEN THE 2ND AND 10TH LOAD CYCLES AFTER STAPLE INSERTION IN FLEXION/EXTENSION (d.), LATERAL BENDING (e.) AND AXIAL ROTATION (f.).

4.5.3. SMA VS. PROTOTYPE STAPLE:

Analysis revealed a significant difference between the control measurements of stiffness of the SMA and Prototype staple groups (before staple insertion) in all three axes of movement; flexion/extension *P*=0.001, lateral bending *P*=0.026 and axial rotation *P*=0.004. This prohibited direct comparison of their post insertion stiffness values. Therefore, the normalized stiffness ratios were used to assess the difference between the two groups.

In flexion/extension the SMA staple produced a construct which was 8% stiffer than the Prototype staple. This difference was statistically insignificant (*P*=0.298). This was maintained in both flexion and extension.

In lateral bending the Prototype staple resulted in a 16% stiffer construct than the SMA staple. This was statistically significant (*P*=0.023). The main difference was in bending away from the staple (to the right) where the Prototype group were 42% stiffer than the SMA group (*P*=0.003). This was in contrast to bending towards the staple (to the left) where the Prototype group were 3% less stiff than the SMA group (*P*=0.643).

In axial rotation the Prototype group were 7% less stiff than the SMA group, however this not statistically significant (*P*=0.372). This difference was maintained in both left and right axial rotation.

4.5.4. SINGLE AXIS ANALYSIS OF THE EFFECT OF STAPLE INSERTION:

When testing a single motion segment in a single axis of movement (flexion/extension, lateral bending or axial rotation) the changes in stiffness between the tenth load cycle pre and post staple insertion were as follows:

In flexion/extension alone the SMA staple caused an overall reduction in stiffness of 10%. This was slightly more in flexion than extension. The Prototype staple caused a minimal decrease in stiffness of 4%. However, this was the result of an opposing effect in which the prototype staple caused a *reduction* of stiffness in flexion of 25% and an *increase* in stiffness in extension of 29%.

In lateral bending alone the SMA staple caused a 43% drop in stiffness. Bending towards the staple reduced the stiffness by 44% and bending away from the staple reduced it by 41%. The Prototype staple on the other hand reduced the stiffness by 16%. This was achieved by a reduction of 15% when bending towards the staple and 17% when bending away from it.

In axial rotation alone the SMA staple insertion caused a reduction in stiffness of 27%. This was marginally more in the direction of movement towards the staple. The Prototype staple however, caused an increase in stiffness by 14%. This was mainly in the direction away from the staple where it increased by 22%.

4.6. MICROCT FINDINGS:

The motion segments were graded according to the number of epiphyses with prong tracks after staple insertion. Grade 2 involves both the cephalic and caudal epiphyses. Grade 1 involves one of either the cephalic or caudal epiphysis. Grade 0 involves neither epiphysis.

It was found that 15 (55.6%) were grade 2 insertions, while 10 (37%) were grade 1 and 2 (7.4%) were grade 0. In other words, in more than half of the staple insertions performed in this study, the staple tips penetrated both epiphyses.

There was a near significant difference between the volume (**L**ength x **W**idth x **H**eight) of bone destruction from each prong in grades 1 and 2 with a higher volume in grade 2 by 20% (P=0.058). Due to the fact that the length of the inserted staple is operator dependent, the cross section area of the staple prongs (WxH) was used to study any relationship between the insertion grade and the amount of bone destruction. The overall cross-sectional area of bone destruction from the prongs was 24% larger in the grade 2 group compared to the grade 1 group, which was statistically significant (P=0.022). Looking at each staple type independently shows that within the SMA staple group the grade 2 insertion group had a 0.4% larger cross section than the grade 1 group. This was insignificant (P=0.961). Within the Prototype group the grade 2 insertion group had a 7.8% smaller cross section than the grade 1 group, however, this was still insignificant (P=0.587).

Also comparing the cross-sectional area of bone destruction of the Prototype and SMA groups showed 44% larger total cross-section bone destruction in the Prototype group than the SMA group. This was highly significant (*P*<0.001). This significance was maintained after adjusting for grade of insertion.

It was also interesting to note that on visual assessment of the Micro CT films the main trabecular damage appeared to be on the outer surface of the staple prongs (Figure 32) in all the samples and both staple types.

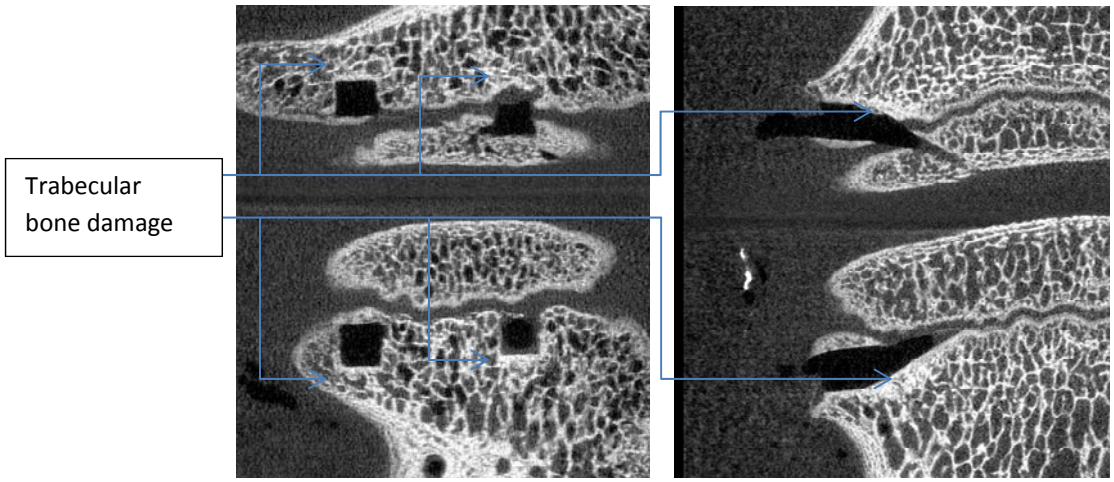

FIGURE 32: MICRO CT SHOWING STAPLE PRONG TRACKS HIGHLIGHTING SITE OF TRABECULAR BONE DAMAGE.

4.7. The Effect of Staple Insertion Grade on Stiffness

Due to the variability in individual specimen control stiffness (pre-staple insertion) and the small number of specimens the normalized stiffness ratios (k/k0) were used to assess the differences between staple insertion grades. There was an insignificant difference between the overall stiffness ratios in both groups (*P*=0.691). Grade 2 spines had higher stiffness ratios than grade 1 spines in lateral bending with a significant increase of 23% (*P*=0.002). In flexion/extension there was an increase in stiffness ratios by 3% and in axial rotation there was a decrease in stiffness ratios by 12% which was not significant (*P*=0.967 and *P*=0.144 respectively).

Looking at the SMA staples alone, there were nine (65%) segments with grade 1 staple insertions and five (35%) segments with grade 2 insertions. There were no grade 0 staples. There was no significant

difference between the stiffness ratios in both groups. There was no significant difference for the ratios of either grade. However, it was near significant in lateral bending with an increase of 17% (*P*=0.096).

In the Prototype staple group there were two grade 0 insertions (15%), one grade 1 insertion (8%) and ten grade 2 insertions (77%). There was a 7% higher stiffness ratio in the mean grade 2 group segments than the mean stiffness ratio of the other segments but this was not significant (*P*=0.167). However it was near significant in lateral bending with a 21% increase in stiffness ratio (*P*=0.095).

5. DISCUSSION

The aim of this study was to assess the effect of two fusionless implant designs (vertebral body staples) on the biomechanics of thoracic vertebral motion segments, with a focus on how vertebral body staples alter the stiffness of the motion segment, and the extent to which they create local tissue damage during repeated load cycling. This work was motivated by the current uncertainty in *in vivo* studies regarding the extent to which vertebral body staples are capable of correcting scoliosis, as well as a previous biomechanical study in the author's group which (under displacement controlled testing) showed a decrease in motion segment stiffness following staple insertion, which appeared to run contrary to the expected stiffening effect of a metallic implant bridging the adjacent vertebral bodies.

In order to allow reliable comparison of the results obtained with those from other studies, it was necessary to carefully assess the effects of various testing conditions on the resulting stiffness values. Owing to their similarity to human spines, immature bovine (calf) spines have been previously suggested as an appropriate model for the young human spine (Cotterill et al., 1986, Kettler et al., 2007, Swartz et al., 1991, Wilke et al., 1996, Wilke et al., 1997), and were chosen for the current study. Aside from differences between research groups in the design of the spine testing equipment used (moment or displacement control), another important potential source of variability between and within studies is the testing protocol itself, particularly with regard to: the amount of force applied, the number of times a particular motion segment is loaded (i.e. the cumulative number of loading cycles) (Wilke et al., 1996, Shillington et al., 2011, Panjabi et al., 1981), the level of dissection and also whether the same motion segment is tested on successive days by freezing and re-thawing. Therefore, as part of the current study, the effects of these testing variables on motion segment stiffness in the immature bovine thoracic spine were characterised.

In regards to the moment applied, this study showed that with the spinous processes and costovertebral as well as costotransverse joints intact the average moment required to achieve $\pm 6^{o}$ of motion in flexion/extension was lower than other previous studies (Riley et al., 2004, Wilke et al., 1996). This could be attributed to the lack of axial preload as well as differences in testing temperature and humidity.

As for the effect of the number of cumulative load cycles, the results showed statistically significant decreases in motion segment stiffness in two of the three loading directions (22% decrease in flexion/extension, 18% decrease in lateral bending, and no significant change in axial rotation) between the 3rd and 500th load cycles. However, the results suggest that calf thoracic spine segments can be tested for up to 200 cycles with minimal change in stiffness, but beyond 200 cycles, caution should be used in interpreting the results as the changes in stiffness are appreciable.

To the best of the author's knowledge there has only been one previous study examining the effect of repeated cyclic loading on motion segment stiffness, and this was performed in axial rotation only on mature sheep spines, loaded to ±5Nm to a maximum of 500 loading cycles (Wilke et al., 1998a). This prior study did not find any change in axial rotation stiffness, which agrees with the finding of our current study for axial rotation.

The level of dissection test showed a significant decrease in motion segment stiffness after excision of the costovertebral joints in flexion/extension of 18%. The effect of further excision of the spinous process was minimal. Lateral bending was affected with both dissection of the costovertebral joints and spinous process with a reduction in stiffness of 13% and 5% respectively. Axial rotation stiffness was affected to a much lesser degree with only a 6.5% drop in stiffness.

To the best of the author's knowledge there haven't been any published studies examining the biomechanical effect of excising the costovertebral joints alone or with the spinous processes. This segment of the study was designed specifically to answer this question and allow for these effects to be used when comparing previous different studies and designing studies in the future.

As for the effect of multiple freeze-thaw cycles there was a relatively large (30%) statistically significant increase in lateral bending stiffness after 5 freeze-thaw cycles, but no statistically significant changes in flexion/extension or axial rotation.

A recent study (Tan and Uppuganti, 2012) found that flexibility increased (reduced stiffness) in motion segments of a mature (elderly) human cadaver lumbar spine subjected to repeated freeze/thaw cycles. This was tested with a moment of ±7.5Nm in all primary directions of flexion/extension, lateral bending and axial rotation with measurements taken at the fifth cycle. Hongo *et al*. (Hongo et al.,

2008) explored the effect of freeze thaw cycles on the biomechanics of porcine lumbar motion segments under an applied moment of ±5Nm with three freeze-thaw cycles. These authors found that after the initial freeze there was no significant change for subsequent freeze-thaw cycles. Although my findings agree with this in flexion/extension and axial rotation, I found a difference between the effects of repeated freeze-thaw cycles on flexion and extension stiffness when the two loading directions were assessed individually. Flexion stiffness was not significantly affected; however extension stiffness was. In lateral bending, my results run counter to those of both previous studies, as a significant increase in stiffness was recorded. However, I note that the elderly human lumbar spine tested by Tan and Uppuganti et al. may have been more prone to damage than the healthy immature bovine thoracic spines used in the current study. As is seen in Figure 31, the changes in stiffness that occurred between the first and second freeze/thaw cycles were often larger than the changes occurring between pairs of subsequent freezing cycles, however these 1st to 2nd freeze cycle changes were only statistically significant for axial rotation. Since freezing temperatures were constant for each cycle, it seems reasonable that the largest stiffness changes would occur the first time that any micro-structural damage caused by ice crystal formation within the tissue was subjected to loading, i.e. between the first and second cycles (Clavert et al., 2001).

The findings of these tests show that bending movements are more susceptible than axial rotation to testing environments. I speculate that this is related to the stabilising ligaments of the spine. These are mainly oriented in a longitudinal or oblique fashion with the thickest ligaments oriented in a longitudinal direction. As a result any change in stiffness of these ligaments will affect the bending movements more than axial rotation (Giannini et al., 2008, Ng et al., 2005).

The main part of this study, assessing the effect of vertebral body staple insertion on motion segment stiffness, concurs with the previous study by Shillington, where displacement control was used (Shillington et al., 2011). The motion segment stiffness was reduced in all three main axes of movement following staple insertion. The least affected movement was flexion/extension. Lateral bending was the most affected direction of movement with a significant drop in stiffness. This was most noted when bending away from the staple. This decrease in stiffness is contrary to what one would expect from such a construct. It also is contrary to what Puttlitz *et al*. (Puttlitz et al., 2007) described with a reduction in range of motion of the test segment; which implies an increase in

stiffness. However, the testing was performed over a single load cycle with an indeterminant loading rate of 1Nm increments. This makes a direct comparison difficult. Although our findings concur with Zhang *et al*. (Zhang et al., 2013), the significance of the reduction in stiffness was different from our findings. This could be attributed to the fact that multiple levels were used (T6-T11).

When studying the effect of single axis movement the results indicate a greater effect on the motion segment stiffness especially in lateral bending and axial rotation. There are two explanations for this. First: The effect of sequential testing (flexion/extension followed by lateral bending and then axial rotation). Second: Small sample size. Each axis was tested on a single motion segment only. Therefore the sample may not be representative.

Comparing different staple designs reveals that staple design and/or material play a role in the stiffness of the construct. However this was significant in lateral bending only. Despite this difference, the prototype group followed the same trend of a reduction in motion segment stiffness as found in the SMA staple. In both staple types the effects were evident after the first load cycle.

The micro-CT findings revealed physeal damage in all the specimens on staple insertion and subsequent cyclic loading. The results suggest that insertion into the bone without compromise of the physis produces a larger reduction in stiffness as the bone experiences more damage in comparison to separation of the epiphysis. This could be attributed to the difference in rigidity between the trabecular bone and epiphyseal cartilage. It may also explain the drop in staple body load as demonstrated by Shillington *et al*. (Shillington et al., 2011) over 5 load cycles. Damage to the physis could result in convex epiphyseal growth arrest which would contribute to scoliosis correction. However, it is unclear how much of the compression effect on the physis (the Hueter-Volkmann law) might contribute to the scoliosis correction as compared to the physeal damage (hemiepiphysiodesis) as demonstrated by Carreau *et al.* in histology assessment of the epiphyses (Carreau et al., 2012).

The findings on micro-CT confirm the findings of Shillington *et al*. regarding the pattern of trabecular bone damage. All of the motion segments show trabecular damage limited to the outer surface of the staple prongs indicating that this damage occurred during staple insertion rather than during subsequent loading, although it is noteworthy that the rapid drop in staple force observed by Shillington *et al*. over only five load cycles was attributed to tissue damage caused by the staple tips.

There was no visible trabecular damage on the inner surface of the prongs that would indicate compression resulting from the shape memory function of the staples. As the staples are inserted cold the staple prongs flex to the closed position due to the bending load created by the chamfer at the end of the prong tips. As the staples warm up they maintain this shape as it is the same as the original memory shape of the staple; this memory shape of the staple, however, may help reduce the incidence of staple back out. This correlates with the findings in the prototype (not made of shape memory alloy) group, as all the staples self-closed on staple insertion via the inbuilt ratchet system.

The finding that despite following the recommended surgical technique for staple insertion, there were variable grades of epiphyseal involvement (grades 0, 1 and 2) is important. This was not reported in previous studies and may well explain the variability in reported results (Betz et al., 2010, O'Leary P et al., 2011, Braun et al., 2005, Guille et al., 2007).

It is difficult to accept that the damage caused by the inserted staple to the vertebral body is sufficient to reduce the stiffness of the motion segment. One hypothesis is that the staple interferes with the annulus fibrosis leading to a lax segment, therefore affecting the properties of the intervertebral disc. As a result this would alter the pivot point of the vertebra as well as the coupled movements with each major axis of movement. I would like to investigate this further by using a 3D optical tracking system to collect the data for the coupled movements as well as the main axis of movement.

There are several limitations to this study. Firstly, a fixed sequence of loading directions was used. All specimens were tested in the order of flexion/extension, then lateral bending followed by axial rotation. It would be of value to ascertain in future whether or not the loading sequence has any significant effect on the measured stiffness, or whether one of the loading directions in isolation is responsible for most of the observed stiffness change. Secondly, the testing was conducted without axial loading of the spine segments. Although axial loading is significant in the lumbar spine, it is unclear as to its significance in the thoracic spine, especially in a quadruped animal model, and therefore was not included in this study. Thirdly, rotation and moment measurements were recorded in the primary loading direction only in this study. Therefore the values of any off-axis coupled moments as well as their significance remain unknown. Further study using a multilevel model and adding 3D stereographic tracking would be of great value to clarify the effect of interventions on coupled movements. Also, further study to assess the effect of restricting the coupled movements on

recorded motion segment stiffness is required. Fourthly, the stiffness was calculated over the region of the moment vs rotation curve between 0.5 and 1Nm. The choice of region would be expected to have some effect on the calculated stiffness value. However as this study was evaluating the change in stiffness with the intervention, and the same moment range was used consistently throughout, this limitation is likely to have an insignificant effect on the results presented here. Finally all specimens were frozen prior to any testing. As a result no fresh specimen testing was conducted and could not be included in this study.

6. CONCLUSION:

Scoliosis correction without any impact on mobility and growth potential is the ideal treatment. Fusionless scoliosis correction surgery techniques have evolved pursuing this ideal. Thoracic vertebral body stapling is a fusionless technique with promising clinical results.

In vitro biomechanical testing of immature bovine thoracic spine segments can be performed up to 200 cycles without significant changes in stiffness. However, when testing protocols require greater than 200 cycles, or when repeated freeze-thaw cycles are involved, it is important to account for the effect of cumulative load cycles especially in flexion/extension or lateral bending. In relation to the degree of spinal segment dissection, the effect on segment stiffness depends on the axis of movement under study. We would also recommend designing the study so as to allow the biomechanical testing to be completed in a single session to minimize the effect of repeated freeze-thaw cycles.

My findings suggest that the clinical results may be due to convex epiphyseal growth arrest. However, further study would be required to determine how much of the compression effect on the physis (the Hueter-Volkmann law) contributes to the scoliosis correction as compared to the physeal damage (hemiepiphysiodesis).

The important result from this study is that vertebral body staple insertion results in an overall reduction in spinal motion segment stiffness. This is most expressed in lateral bending. It also results in physeal and trabecular bone damage resulting in a hemiepiphysiodesis. If physeal preservation is an aim of treatment, I would recommend using a different staple design or fusionless scoliosis correction technology.

7. REFERENCES:

AKBARNIA, B. A. M. D. 2007. Management Themes in Early Onset Scoliosis. *Journal of Bone & Joint Surgery - American Volume,* 89-A Supplement**,** 42-54.

AKYUZ, E., BRAUN, J. T., BROWN, N. A. & BACHUS, K. N. 2006. Static versus dynamic loading in the mechanical modulation of vertebral growth. *Spine,* 31**,** E952-8.

ARONSSON, D. D., STOKES, I. A., ROSOVSKY, J. & SPENCE, H. 1999. Mechanical modulation of calf tail vertebral growth: implications for scoliosis progression. *Journal of spinal disorders,* 12**,** 141-6.

BETZ, R. R., D'ANDREA, L. P., MULCAHEY, M. J. & CHAFETZ, R. S. 2005. Vertebral body stapling procedure for the treatment of scoliosis in the growing child. *Clinical orthopaedics and related research***,** 55-60.

BETZ, R. R., KIM, J., D'ANDREA, L. P., MULCAHEY, M. J., BALSARA, R. K. & CLEMENTS, D. H. 2003. An innovative technique of vertebral body stapling for the treatment of patients with adolescent idiopathic scoliosis: a feasibility, safety, and utility study. *Spine,* 28**,** S255-65.

BETZ, R. R. M. D., RANADE, A. M. D., SAMDANI, A. F. M. D., CHAFETZ, R. D. P. T., D'ANDREA, L. P. M. D., GAUGHAN, J. P. P., ASGHAR, J. M. D., GREWAL, H. M. D. & MULCAHEY, M. J. P. 2010. Vertebral Body Stapling: A Fusionless Treatment Option for a Growing Child With Moderate Idiopathic Scoliosis. *Spine,* 35**,** 169-176.

BLAIR, J., ABITBOL, J.-J. & VACCARO, A. R. 1993. Anterior thoracolumbar instrumentation. *Operative Techniques in Orthopaedics,* 3**,** 243-250.

BLOUNT, W. P. & CLARKE, G. R. 1949. Control of bone growth by epiphyseal stapling; a preliminary report. *The Journal of bone and joint surgery. American volume,* 31A**,** 464-78.

BRAUN, J. T., AKYUZ, E., OGILVIE, J. W. & BACHUS, K. N. 2005. The efficacy and integrity of shape memory alloy staples and bone anchors with ligament tethers in the fusionless treatment of experimental scoliosis. *The Journal of bone and joint surgery. American volume,* 87**,** 2038-51.

BRAUN, J. T., AKYUZ, E., UDALL, H., OGILVIE, J. W., BRODKE, D. S. & BACHUS, K. N. 2006a. Three-dimensional analysis of 2 fusionless scoliosis treatments: a flexible ligament tether versus a rigid-shape memory alloy staple. *Spine,* 31**,** 262-8.

BRAUN, J. T., HOFFMAN, M., AKYUZ, E., OGILVIE, J. W., BRODKE, D. S. & BACHUS, K. N. 2006b. Mechanical modulation of vertebral growth in the fusionless treatment of progressive scoliosis in an experimental model. *Spine,* 31**,** 1314-20.

BRAUN, J. T., OGILVIE, J. W., AKYUZ, E., BRODKE, D. S. & BACHUS, K. N. 2004. Fusionless scoliosis correction using a shape memory alloy staple in the anterior thoracic spine of the immature goat. *Spine,* 29**,** 1980-9.

BRAUN, J. T., OGILVIE, J. W., AKYUZ, E., BRODKE, D. S., BACHUS, K. N. & STEFKO, R. M. 2003. Experimental scoliosis in an immature goat model: a method that creates idiopathic-type deformity with minimal violation of the spinal elements along the curve. *Spine,* 28**,** 2198-203.

BUNNELL, W. P. M. 1986. The Natural History of Idiopathic Scoliosis Before Skeletal Maturity. *Spine,* 11**,** 773-776.

BUSSCHER, I., VAN DER VEEN, A. J., VAN DIEEN, J. H., KINGMA, I., VERKERKE, G. J. & VELDHUIZEN, A. G. 2010. In vitro biomechanical characteristics of the spine: a comparison between human and porcine spinal segments. *Spine,* 35**,** E35-42.

CAMPBELL, R. M., JR. 2013. VEPTR: past experience and the future of VEPTR principles. *Eur Spine J,* 22 Suppl 2**,** S106-17.

CARREAU, J. H., FARNSWORTH, C. L., GLASER, D. A., DOAN, J. D., BASTROM, T., BRYAN, N. & NEWTON, P. O. 2012. The modulation of spinal growth with nitinol intervertebral stapling in an established swine model. *Journal of Children's Orthopaedics,* 6**,** 241-253.

CLAVERT, P., KEMPF, J.-F., BONNOMET, F., BOUTEMY, P., MARCELIN, L. & KAHN, J.-L. 2001. Effects of freezing/thawing on the biomechanical properties of human tendons. *Surgical and Radiologic Anatomy,* 23**,** 259-262.

CLAYSON, D., LUZ-ALTERMAN, S., CATALETTO, M. M. & LEVINE, D. B. 1987. Long-term psychological sequelae of surgically versus nonsurgically treated scoliosis. *Spine,* 12**,** 983-6.

CLIMENT, J. M. & SANCHEZ, J. 1999. Impact of the type of brace on the quality of life of Adolescents with Spine Deformities. *Spine,* 24**,** 1903-8.

COBB, J. R. 1948. Outline for the study of scoliosis. *AAOS Instr Course Lect.,* 5**,** 261–275.

COCHRAN, T., IRSTAM, L. & NACHEMSON, A. 1983. Long-term anatomic and functional changes in patients with adolescent idiopathic scoliosis treated by Harrington rod fusion. *Spine,* 8**,** 576-84.

COE, J. D., ARLET, V., DONALDSON, W., BERVEN, S., HANSON, D. S., MUDIYAM, R., PERRA, J. H. & SHAFFREY, C. I. 2006. Complications in spinal fusion for adolescent idiopathic scoliosis in the new millennium. A report of the Scoliosis Research Society Morbidity and Mortality Committee. *Spine,* 31**,** 345-9.

COTTERILL, P. C., KOSTUIK, J. P., D'ANGELO, G., FERNIE, G. R. & MAKI, B. E. 1986. An anatomical comparison of the human and bovine thoracolumbar spine. *Journal of orthopaedic research,* 4**,** 298-303.

CRAWFORD, C. H. I. I. I. M. D. & LENKE, L. G. M. D. 2010. Growth Modulation by Means of Anterior Tethering Resulting in Progressive Correction of Juvenile Idiopathic Scoliosis: A Case Report. *Journal of Bone & Joint Surgery - American Volume,* 92-A**,** 202-209.

DE VISSER, H., ROWE, C. & PEARCY, M. 2007. A robotic testing facility for the measurement of the mechanics of spinal joints. *Institution of Mechanical Engineers. Proceedings. Part H: Journal of Engineering in Medicine,* 221**,** 221-227.

DIEDRICH, O., VON STREMPEL, A., SCHLOZ, M., SCHMITT, O. & KRAFT, C. N. 2002. Long-term observation and management of resolving infantile idiopathic scoliosis: A 25-YEAR FOLLOW-UP. *Journal of Bone & Joint Surgery - British Volume,* 84-B**,** 1030-1035.

DRESPE, I. H., POLZHOFER, G. K., TURNER, A. S. & GRAUER, J. N. 2005. Animal models for spinal fusion. *The spine journal,* 5**,** 209S-216S.

DWYER, A. F. 1973. Experience of Anterior Correction of Scoliosis. *Clinical Orthopaedics & Related Research June,* 93**,** 191-206.

DWYER, A. F., NEWTON, N. C. & SHERWOOD, A. A. 1969. An anterior approach to scoliosis. A preliminary report. *Clin Orthop Relat Res,* 62**,** 192-202.

FERNANDES, P. M. D. & WEINSTEIN, S. L. M. D. 2007. Natural History of Early Onset Scoliosis. *Journal of Bone & Joint Surgery - American Volume,* 89-A Supplement**,** 21-33.

FRYMOYER, J. W. & WIESEL, S. W. 2004. *The adult and pediatric spine,* Philadelphia, Lippincott Williams & Wilkins.

GEERVLIET, P. C., VAN ROYEN, B. J., VONK NOORDEGRAAF, A., KRANENDONK, S. E., DAVID, E. F. & PAUL, M. A. 2007. Late spontaneous hemothorax complicating anterior spinal instrumentation in adolescent idiopathic scoliosis. *Spine,* 32**,** E730-3.

GIANNINI, S., BUDA, R., DI CAPRIO, F., AGATI, P., BIGI, A., DE PASQUALE, V. & RUGGERI, A. 2008. Effects of freezing on the biomechanical and structural properties of human posterior tibial tendons. *Int Orthop,* 32**,** 145-51.

GILBERTSON, L. G., DOEHRING, T. C. & KANG, J. D. 2000. New methods to study lumbar spine biomechanics: Delineation of in vitro load-displacement characteristics by using a robotic/UFS testing system with hybrid control. *Operative Techniques in Orthopaedics,* 10**,** 246-253.

GOEL, V. K., WILDER, D. G., POPE, M. H. & EDWARDS, W. T. 1995. Controversy Biomechanical Testing of the Spine: Load-Controlled Versus Displacement-Controlled Analysis. *Spine,* 20**,** 2354-2357.

GOLDSTEIN, L. A. M. D. 1971. The Surgical Management of Scoliosis. *Clinical Orthopaedics & Related Research June,* 77**,** 32-56.

GORE, D. R., PASSEHL, R., SEPIC, S. & DALTON, A. 1981. Scoliosis screening: results of a community project. *Pediatrics,* 67**,** 196-200.

GUILLE, J. T., D'ANDREA, L. P. & BETZ, R. R. 2007. Fusionless treatment of scoliosis. *The Orthopedic clinics of North America,* 38**,** 541-5, vii.

HACQUEBORD, J. H. & LEOPOLD, S. S. 2012. In Brief: The Risser Classification: A Classic Tool for the Clinician Treating Adolescent Idiopathic Scoliosis. *Clinical Orthopaedics and Related Research,* 470**,** 2335-2338.

HALM, H. 2000. [Ventral and dorsal correcting and stabilizing methods in idiopathic scoliosis. Long-term outcome]. *Orthopade,* 29**,** 543-62.

HALM, H., RICHTER, A., THOMSEN, B., KOSZEGVARY, M., AHRENS, M. & QUANTE, M. 2009. [Anterior scoliosis surgery. State of the art and a comparison with posterior techniques]. *Orthopade,* 38**,** 131-4, 136-40, 142-5.

HARRINGTON, P. R. 1962. Treatment of scoliosis. Correction and internal fixation by spine instrumentation. *J Bone Joint Surg Am,* 44-A**,** 591-610.

HARRINGTON, P. R. 1977. The etiology of idiopathic scoliosis. *Clinical orthopaedics and related research***,** 17-25.

HASLER, C. C., MEHRKENS, A. & HEFTI, F. 2010. Efficacy and safety of VEPTR instrumentation for progressive spine deformities in young children without rib fusions. *Eur Spine J,* 19**,** 400-8.

HAWES, M. C. & O'BRIEN J, P. 2006. The transformation of spinal curvature into spinal deformity: pathological processes and implications for treatment. *Scoliosis,* 1**,** 3.

HERKOWITZ, H. N., GARFIN, S. R., EISMONT, F. J., BELL, G. R. & BALDERSTON, R. A. 2011. Idiopathic Scoliosis. *Rothman-Simeone The Spine.* 6th ed.: Saunders.

HONGO, M., GAY, R. E., HSU, J. T., ZHAO, K. D., ILHARREBORDE, B., BERGLUND, L. J. & AN, K. N. 2008. Effect of multiple freeze-thaw cycles on intervertebral dynamic motion characteristics in the porcine lumbar spine. *Journal of biomechanics,* 41**,** 916-20.

HOWARD, A., WRIGHT, J. G. & HEDDEN, D. 1998. A comparative study of TLSO, Charleston, and Milwaukee braces for idiopathic scoliosis. *Spine,* 23**,** 2404-11.

HUETER, C. 1862. Anatomische Studien an den Extremitätengelenken Neugeborener und Erwachsener. *Archiv für pathologische Anatomie und Physiologie und für klinische Medicin,* 25**,** 572-599.

IZATT, M. T., HARVEY, J. R., ADAM, C. J., FENDER, D., LABROM, R. D. & ASKIN, G. N. 2006. Recovery of pulmonary function following endoscopic anterior scoliosis correction: evaluation at 3, 6, 12, and 24 months after surgery. *Spine,* 31**,** 2469-77.

JAMES, J. I. P. M. S. F. R. C. S. 1971. Infantile Idiopathic Scoliosis. *Clinical Orthopaedics & Related Research June,* 77**,** 57-72.

KANE, W. J. 1977. Scoliosis prevalence: a call for a statement of terms. *Clinical orthopaedics and related research***,** 43-6.

KETTLER, A., LIAKOS, L., HAEGELE, B. & WILKE, H. J. 2007. Are the spines of calf, pig and sheep suitable models for pre-clinical implant tests? *European spine journal,* 16**,** 2186-92.

KOHLER, R., GALLAND, O., MECHIN, H., MICHEL, C. R. & ONIMUS, M. 1990. The Dwyer procedure in the treatment of idiopathic scoliosis. A 10-year follow-up review of 21 patients. *Spine (Phila Pa 1976),* 15**,** 75-80.

LAST, R. J. & MCMINN, R. M. H. 1994. *Last's anatomy, regional and applied,* Edinburgh ; New York, Churchill Livingstone.

LAVELLE, W. F., SAMDANI, A. F., CAHILL, P. J. & BETZ, R. R. 2011. Clinical outcomes of nitinol staples for preventing curve progression in idiopathic scoliosis. *Journal of pediatric orthopedics,* 31**,** S107-13.

LEE, C. S., CHUNG, S. S., SHIN, S. K., PARK, Y. S., PARK, S. J. & KANG, K. C. 2011. Changes of Upper Thoracic Curve and Shoulder Balance in Thoracic Adolescent Idiopathic Scoliosis Treated by Anterior Selective Thoracic Fusion Using VATS. *Journal of spinal disorders & techniques*.

LENKE, L. G. M. D. & DOBBS, M. B. M. D. 2007. Management of Juvenile Idiopathic Scoliosis. *Journal of Bone & Joint Surgery - American Volume,* 89-A Supplement**,** 55-63.

LINDE, F., HVID, I. & PONGSOIPETCH, B. 1989. Energy absorptive properties of human trabecular bone specimens during axial compression. *J Orthop Res,* 7**,** 432-9.

LLOYD-ROBERTS, G. C. & PILCHER, M. F. 1965. STRUCTURAL IDIOPATHIC SCOLIOSIS IN INFANCY: A Study of the Natural History of 100 Patients. *Journal of Bone & Joint Surgery, British Volume,* 47-B**,** 520-523.

LONNER, B. S. 2007. Emerging minimally invasive technologies for the management of scoliosis. *Orthop Clin North Am,* 38**,** 431-40; abstract vii-viii.

LONSTEIN, J. E. & WINTER, R. B. 1994. The Milwaukee brace for the treatment of adolescent idiopathic scoliosis. A review of one thousand and twenty patients. *The Journal of bone and joint surgery. American volume,* 76**,** 1207-21.

MARKS, D., IQBAL, M., THOMPSON, A. & PIGGOTT, H. 1996. Convex spinal epiphysiodesis in the management of progressive infantile idiopathic scoliosis. *Spine,* 21**,** 1884 - 1888.

MARUYAMA, T. & TAKESHITA, K. 2008. Surgical treatment of scoliosis: a review of techniques currently applied. *Scoliosis,* 3**,** 6.

MCCARROLL, H. R. & COSTEN, W. 1960. *Attempted Treatment of Scoliosis by Unilateral Vertebral Epiphyseal Arrest*.

MENTE, P. L., STOKES, I. A., SPENCE, H. & ARONSSON, D. D. 1997. Progression of vertebral wedging in an asymmetrically loaded rat tail model. *Spine (Phila Pa 1976),* 22**,** 1292-6.

MOE, J. H. & KETTLESON, D. N. 1970. Idiopathic scoliosis. Analysis of curve patterns and the preliminary results of Milwaukee-brace treatment in one hundred sixty-nine patients. *The Journal of bone and joint surgery. American volume,* 52**,** 1509-33.

NACHLAS, I. W. & BORDEN, J. N. 1951. The cure of experimental scoliosis by directed growth control. *J Bone Joint Surg Am,* 33**,** 24-34.

NETTER, F. H. 2010. *Netter Basic Science : Atlas of Human Anatomy : With Student Consult Online Access (5th Edition),* Saint Louis, MO, USA, A Saunders Title.

NEWTON, P. O., FARNSWORTH, C. L., FARO, F. D., MAHAR, A. T., ODELL, T. R., MOHAMAD, F., BREISCH, E., FRICKA, K., UPASANI, V. V. & AMIEL, D. 2008a. Spinal growth modulation with an anterolateral flexible tether in an immature bovine model: disc health and motion preservation. *Spine (Phila Pa 1976),* 33**,** 724-33.

NEWTON, P. O., FRICKA, K. B., LEE, S. S., FARNSWORTH, C. L., COX, T. G. & MAHAR, A. T. 2002. Asymmetrical flexible tethering of spine growth in an immature bovine model. *Spine (Phila Pa 1976),* 27**,** 689-93.

NEWTON, P. O., UPASANI, V. V., FARNSWORTH, C. L., OKA, R., CHAMBERS, R. C., DWEK, J., KIM, J. R., PERRY, A. & MAHAR, A. T. 2008b. Spinal growth modulation with use of a tether in an immature porcine model. *J Bone Joint Surg Am,* 90**,** 2695-706.

NG, B. H., CHOU, S. M., LIM, B. H. & CHONG, A. 2005. The changes in the tensile properties of tendons after freeze storage in saline solution. *Proc Inst Mech Eng H,* 219**,** 387-92.

NILSONNE, U. 1969. Vertebral Epiphyseodesis of the Thoracic Curve in the Operative Treatment of Idiopathic Scoliosis. *Acta Orthopaedica,* 40**,** 237-245.

NOONAN, K. J., WEINSTEIN, S. L., JACOBSON, W. C. & DOLAN, L. A. 1996. Use of the Milwaukee brace for progressive idiopathic scoliosis. *The Journal of bone and joint surgery. American volume,* 78**,** 557-67.

O'LEARY P, T., STURM, P. F., HAMMERBERG, K. W., LUBICKY, J. P. & MARDJETKO, S. M. 2011. Convex hemiepiphysiodesis: the limits of vertebral stapling. *Spine,* 36**,** 1579-83.

ODA, I., ABUMI, K., CUNNINGHAM, B. W., KANEDA, K. & MCAFEE, P. C. 2002. An in vitro human cadaveric study investigating the biomechanical properties of the thoracic spine. *Spine,* 27**,** E64-70.

ODA, I., ABUMI, K., LU, D., SHONO, Y. & KANEDA, K. 1996. Biomechanical role of the posterior elements, costovertebral joints, and rib cage in the stability of the thoracic spine. *Spine,* 21**,** 1423-9.

PANJABI, M. M. 1988. Biomechanical Evaluation of Spinal Fixation Devices: I. A Conceptual Framework. *Spine,* 13**,** 1129-1134.

PANJABI, M. M. 2007. Hybrid multidirectional test method to evaluate spinal adjacent-level effects. *Clinical Biomechanics,* 22**,** 257-265.

PANJABI, M. M., BRAND, R. A., JR. & WHITE, A. A., 3RD 1976. Mechanical properties of the human thoracic spine as shown by three-dimensional load-displacement curves. *The Journal of bone and joint surgery. American volume,* 58**,** 642-52.

PANJABI, M. M., HAUSFELD, J. N. & WHITE, A. A., 3RD 1981. A biomechanical study of the ligamentous stability of the thoracic spine in man. *Acta orthopaedica Scandinavica,* 52**,** 315-26.

PANJABI, M. M. & WHITE, A. A., 3RD 1980. Basic biomechanics of the spine. *Neurosurgery,* 7**,** 76-93.

PUTTLITZ, C. M., MASARU, F., BARKLEY, A., DIAB, M. & ACAROGLU, E. 2007. A biomechanical assessment of thoracic spine stapling. *Spine,* 32**,** 766-71.

RILEY, L. H., 3RD, ECK, J. C., YOSHIDA, H., KOH, Y. D., YOU, J. W. & LIM, T. H. 2004. A biomechanical comparison of calf versus cadaver lumbar spine models. *Spine,* 29**,** E217-20.

RISSER, J. C. M. D. 1958. The Iliac Apophysis: An Invaluable Sign in the Management of Scoliosis. *Clinical Orthopaedics,* 11**,** 111-119.

ROAF, R. 1960. Vertebral growth and its mechanical control. *J Bone Joint Surg Br,* 42-B**,** 40-59.

ROAF, R. 1963. THE TREATMENT OF PROGRESSIVE SCOLIOSIS BY UNILATERAL GROWTH-ARREST. *Journal of Bone & Joint Surgery, British Volume,* 45-B**,** 637-651.

ROTHMAN, R. H. & SIMEONE, F. A. 1992. *The Spine,* Philadelphia, Saunders.

SAMDANI, A. F. M. D., AMES, R. J. B. A., KIMBALL, J. S. B. S., PAHYS, J. M. M. D., GREWAL, H. M. D., PELLETIER, G. J. M. D. & BETZ, R. R. M. D. 2014. Anterior Vertebral Body Tethering for Idiopathic Scoliosis: Two-Year Results. *Spine,* 39**,** 1688-1693.

SHENG, S. R., WANG, X. Y., XU, H. Z., ZHU, G. Q. & ZHOU, Y. F. 2010. Anatomy of large animal spines and its comparison to the human spine: a systematic review. *European spine journal,* 19**,** 46-56.

SHILLINGTON, M. P., LABROM, R. D., ASKIN, G. N. & ADAM, C. J. 2011. A biomechanical investigation of vertebral staples for fusionless scoliosis correction. *Clinical biomechanics,* 26**,** 445-51.

SMIT, T. H. 2002. The use of a quadruped as an in vivo model for the study of the spine - biomechanical considerations. *European spine journal,* 11**,** 137-44.

SMITH, A. D., VON LACKUM, W. H. & WYLIE, R. 1954. *AN OPERATION FOR STAPLING VERTEBRAL BODIES IN CONGENITAL SCOLIOSIS*.

STANDRING, S. 2008. Gray's anatomy. *The anatomical basis of clinical practice,* 3**,** 763-773.

STOKES, I. A. 1994. Three-dimensional terminology of spinal deformity. A report presented to the Scoliosis Research Society by the Scoliosis Research Society Working Group on 3-D terminology of spinal deformity. *Spine (Phila Pa 1976),* 19**,** 236-48.

STOKES, I. A. 2002. Mechanical effects on skeletal growth. *J Musculoskelet Neuronal Interact,* 2**,** 277-80.

STOKES, I. A., GWADERA, J., DIMOCK, A., FARNUM, C. E. & ARONSSON, D. D. 2005. Modulation of vertebral and tibial growth by compression loading: diurnal versus full-time loading. *Journal of orthopaedic research : official publication of the Orthopaedic Research Society,* 23**,** 188-95.

STOKES, I. A., MENTE, P. L., IATRIDIS, J. C., FARNUM, C. E. & ARONSSON, D. D. 2002. Enlargement of growth plate chondrocytes modulated by sustained mechanical loading. *The Journal of bone and joint surgery. American volume,* 84-A**,** 1842-8.

STOKES, I. A., SPENCE, H., ARONSSON, D. D. & KILMER, N. 1996. Mechanical modulation of vertebral body growth. Implications for scoliosis progression. *Spine (Phila Pa 1976),* 21**,** 1162-7.

SUCATO, D. J. 2003. Thoracoscopic Anterior Instrumentation and Fusion for Idiopathic Scoliosis. *Journal of the American Academy of Orthopaedic Surgeons,* 11**,** 221-227.

SWARTZ, D. E., WITTENBERG, R. H., SHEA, M., WHITE, A. A., 3RD & HAYES, W. C. 1991. Physical and mechanical properties of calf lumbosacral trabecular bone. *Journal of biomechanics,* 24**,** 1059-68.

TAKEUCHI, T., ABUMI, K., SHONO, Y., ODA, I. & KANEDA, K. 1999. Biomechanical role of the intervertebral disc and costovertebral joint in stability of the thoracic spine. A canine model study. *Spine,* 24**,** 1414-20.

TAN, J. S. & UPPUGANTI, S. 2012. Cumulative multiple freeze-thaw cycles and testing does not affect subsequent within-day variation in intervertebral flexibility of human cadaveric lumbosacral spine. *Spine (Phila Pa 1976),* 37**,** E1238-42.

THOMPSON, R. E., BARKER, T. M. & PEARCY, M. J. 2003. Defining the Neutral Zone of sheep intervertebral joints during dynamic motions: an in vitro study. *Clinical Biomechanics,* 18**,** 89-98.

THOMPSON, R. E., PEARCY, M. J. & BARKER, T. M. 2004. The mechanical effects of intervertebral disc lesions. *Clin Biomech (Bristol, Avon),* 19**,** 448-55.

TROBISCH, P. D., SAMDANI, A., CAHILL, P. & BETZ, R. R. 2011. Vertebral body stapling as an alternative in the treatment of idiopathic scoliosis. *Operative Orthopadie und Traumatologie,* 23**,** 227-31.

VOLKMANN, R. 1862. Chirurgische Erfahrungen über Knochenverbiegungen und Knochenwachsthum. *Archiv für pathologische Anatomie und Physiologie und für klinische Medicin,* 24**,** 512-540.

WESTRICK, E. R. & WARD, W. T. 2011. Adolescent idiopathic scoliosis: 5-year to 20-year evidence-based surgical results. *Journal of pediatric orthopedics,* 31**,** S61-8.

WICKERS, F. C., BUNCH, W. H. & BARNETT, P. M. 1977. Psychological factors in failure to wear the Milwaukee brace for treatment of idiopathic scoliosis. *Clinical orthopaedics and related research*, 62-6.

WILKE, H. J., JUNGKUNZ, B., WENGER, K. & CLAES, L. E. 1998a. Spinal segment range of motion as a function of in vitro test conditions: effects of exposure period, accumulated cycles, angular-deformation rate, and moisture condition. *The Anatomical record,* 251**,** 15-9.

WILKE, H. J., KRISCHAK, S. & CLAES, L. 1996. Biomechanical comparison of calf and human spines. *Journal of orthopaedic research : official publication of the Orthopaedic Research Society,* 14**,** 500-3.

WILKE, H. J., KRISCHAK, S. T., WENGER, K. H. & CLAES, L. E. 1997. Load-displacement properties of the thoracolumbar calf spine: experimental results and comparison to known human data. *European spine journal,* 6**,** 129-37.

WILKE, H. J., WENGER, K. & CLAES, L. 1998b. Testing criteria for spinal implants: recommendations for the standardization of in vitro stability testing of spinal implants. *European Spine Journal,* 7**,** 148-154.

YAZICI, M. & EMANS, J. 2009. Fusionless instrumentation systems for congenital scoliosis: expandable spinal rods and vertical expandable prosthetic titanium rib in the management of congenital spine deformities in the growing child. *Spine,* 34**,** 1800-7.

ZHANG, W., ZHANG, Y., ZHENG, G., ZHANG, R. & WANG, Y. 2013. A biomechanical research of growth control of spine by shape memory alloy staples. *Biomed Res Int,* 2013**,** 384894.

8. APPENDIX:

8.1. PUBLICATIONS AND PRESENTATIONS ARISING FROM THIS STUDY

- Oral presentation at The Spine Society of Australia 24th Annual Scientific Meeting 19-21 April 2013 titled: “THE EFFECT OF TESTING PROTOCOL ON IMMATURE BOVINE THORACIC SPINE SEGMENT STIFFNESS”

- Poster presentation at The Spine Society of Australia 25th Annual Scientific Meeting 11 - 12 April 2014 titled: “THE ROLE OF THE COSTOVERTEBRAL JOINTS AND SPINOUS PROCESSES IN THORACIC SPINE STABILITY” which won the Best Poster Award

- Poster presentation at The Spine Society of Australia 25th Annual Scientific Meeting 11 - 12 April 2014 titled: “THE EFFECT OF INTERVERTEBRAL STAPLE INSERTION ON BOVINE SPINE SEGMENT STIFFNESS”

- Poster presentation at The Spine Society of Australia 25th Annual Scientific Meeting 11 - 12 April 2014 titled: “INTERVERTEBRAL STAPLE GRADING SYSTEM WITH MICRO-CT”

- Publication: Journal of Engineering in Medicine

  Sunni N, Askin GN, Labrom RD, Izatt MT, Pearcy MJ and Adam CJ. The effect of repeated loading and freeze-thaw cycling on immature bovine thoracic motion segment stiffness. Proc Inst Mech Eng H. 2014; 228: 1100-7.